Effect of over-expressed shati on DA uptake in PC12 cells

We have previously demonstrated that shati-AS, which inhibits the expression of shati mRNA, significantly potentiates the METH-induced decrease in synaptosomal and vesicular [^{3}H] DA uptake compared with that in the shati-SC or CSF-treated mice (Niwa *et al.* 2007a). Moreover, [^{3}H] DA uptake in saline-treated mice was also decreased by shati-AS compared with that in the CSF-treated mice, although shati-SC had no effect on [^{3}H] DA uptake (Niwa *et al.* 2007a). Given the results for synaptosomal and vesicular [^{3}H] DA uptake using shati-AS, we concluded that shati plays a critical role in modulating DA uptake. To address this issue, we investigated the role of shati in DA uptake in PC12 cells transfected with the vector containing shati cDNA.

Transfection of the vector containing shati cDNA increased shati mRNA expression compared with the mock-transfection, suggesting that shati was over-expressed in these cells (Fig. 5a left two columns). The increase in the levels of shati mRNA expression evoked by METH treatment (1 μM, 30 min) in mock-transfected cells was significantly potentiated by shati over-expression in PC12 cells (drug, $F_{1,28} = 20.917$, $p < 0.01$; transfection, $F_{1,28} = 247.684$, $p < 0.01$; drug × transfection, $F_{1,28} = 0.003$, $p = 0.955$; two-way ANOVA) (Fig. 5a right two columns).

We examined the *in vitro* effect of over-expressed shati on [^{3}H] DA uptake in PC12 cells. Shati-over-expressing cells themselves showed increased [^{3}H] DA uptake compared with the mock-transfected cells, suggesting that shati itself promotes DA uptake (Fig. 5b left two columns). We pre-treated PC12 cells with METH (1 μM) for 30 min, and then assayed the uptake of [^{3}H] DA. As shown in Fig. 5b, METH (1 μM, 30 min) decreased [^{3}H] DA uptake compared with the mock-transfected control cells. In the shati-over-expressing cells, the METH-induced decrease in [^{3}H] DA uptake was significantly inhibited compared with that in the mock-transfected cells (drug, $F_{1,40} = 45.807$, $p < 0.01$; transfection, $F_{1,28} = 21.551$, $p < 0.01$; drug × transfection, $F_{1,28} = 0.001$, $p = 0.971$; two-way ANOVA) (Fig. 5b right two columns). These results indicated that shati could attenuate METH-induced inhibition of DA uptake.

Regulation of TNF-α expression by shati

TNF-α activates synaptosomal and vesicular DA uptake (Nakajima *et al.* 2004). TNF-α and its inducer diminish the METH-induced decrease in DA uptake and inhibit the METH-induced dependence (Nakajima *et al.* 2004; Niwa *et al.* 2007c, e). Moreover, given the findings on [^{3}H] DA uptake obtained using shati-AS (Niwa *et al.* 2007a) and shati-over-expressing cells (Fig. 5b), we hypothesized that shati increased DA uptake by regulating TNF-α. To address this issue, we examined expression levels of TNF-α mRNA after transfection of the vector containing shati cDNA or treatment with shati-AS.

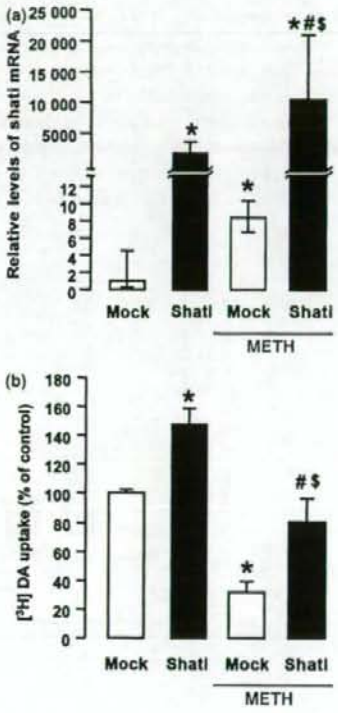

Fig. 5 Effect of overexpression of shati on DA uptake in PC12 cells. (a) Shati mRNA expression in PC12 cells transfected with the vector containing shati cDNA. The mock construct (pcDNA-DEST53), or the vector containing shati cDNA was introduced into PC12 cells. These cells were treated with 1 μM METH for 30 min. Values are means ± SE ($n = 8$). $^*p < 0.05$ versus mock-transfected cells. $^\#p < 0.05$ versus the vector containing shati cDNA-transfected cells. $^\$p < 0.05$ versus METH + mock-transfected cells. (b) Effect of over-expression of shati on [^{3}H] DA uptake in PC12 cells. The mock construct (pcDNA-DEST53), or the vector containing shati cDNA was introduced into PC12 cells. The cells were pre-treated with 1 μM METH for 30 min, and [^{3}H] DA uptake was measured. The [^{3}H] DA uptake was 0.12 ± 0.02 pmol/10 min for the mock-transfected cells. The final concentration of [^{3}H] DA was 20 nM. Values are means ± SE ($n = 10$–12). $^*p < 0.05$ versus mock-transfected cells. $^\#p < 0.05$ versus the vector containing shati cDNA-transfected cells. $^\$p < 0.05$ versus METH + mock-transfected cells.

Shati-over-expressing cells themselves had increased TNF-α mRNA expression compared with the mock-transfected cells (Fig. 6a left two columns), suggesting that shati regulates expression of TNF-α in PC12 cells. The increase in TNF-α mRNA expression evoked by METH treatment (1 μM, 30 min) in mock-transfected cells was significantly potentiated by overexpression of shati *in vitro* (drug, $F_{1,28} = 21.000$, $p < 0.01$; transfection, $F_{1,28} = 65.860$,

$p < 0.01$; drug × transfection, $F_{1,28} = 3.557$, $p = 0.070$; two-way ANOVA) (Fig. 6a right two columns). As shown in Fig. 6b right three columns, the increase in TNF-α mRNA expression evoked by repeated METH treatment in the NAc was significantly abolished by shati-AS, although shati-SC had no effect. Moreover, TNF-α mRNA expression in the NAc of saline-treated mice was also inhibited by shati-AS, although not by shati-SC (drug, $F_{1,47} = 48.473$, $p < 0.01$; intracerebroventricular treatment, $F_{2,47} = 15.670$, $p < 0.01$; drug × intracerebroventricular treatment, $F_{2,47} = 0.239$, $p = 0.788$; two-way ANOVA) (Fig. 6b left three columns), indicating that shati-AS decreases effectively the expression of TNF-α mRNA through the down-regulation of shati mRNA expression.

As shown in Fig. 6c, right four columns, the ameliorative effect of shati on the METH-induced decrease in DA uptake

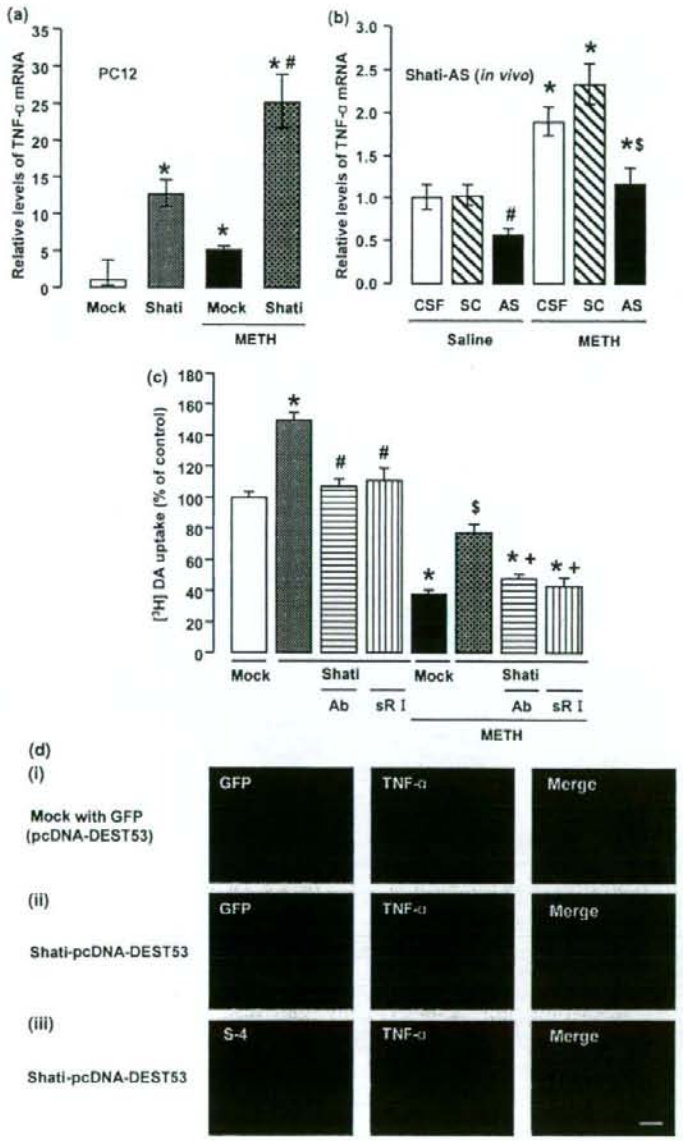

was antagonized by treatment with the TNF-αantibody (50 ng/mL) or soluble TNF receptor I (1 ng/mL). The shati-induced potentiation of DA uptake was also inhibited by the treatments in shati-over-expressing cells (drug, $F_{1,72} = 296.090$, $p < 0.01$; transfection, $F_{1,72} = 13.864$, $p < 0.01$; neutralization, $F_{1,72} = 32.930$, $p < 0.01$; drug × transfection, $F_{1,72} = 0.189$, $p = 0.665$; drug × neutralization, $F_{1,72} = 1.496$, $p = 0.225$; transfection × neutralization, $F_{1,72} = 34.828$, $p < 0.01$; drug × transfection × neutralization, $F_{1,72} = 0.003$, $p = 0.958$; three-way ANOVA) (Fig. 6c left four columns). These results suggest that over-expression of shati increased DA uptake by regulating TNF-α in PC12 cells. To confirm the relationship between shati and TNF-α, we examined immunostaining for GFP, which is co-expressed with shati, or S-4 and TNF-α. The cells mock-transfected, which express GFP, but not shati, were immunopositive for GFP, but not TNF-α. The cells transfected with the vector containing shati cDNA, which express both GFP and shati, were immunopositive for GFP or S-4 and TNF-α. The cells immunopositive for S-4 were merged with those positive for TNF-α. These results indicated that shati was expressed in TNF-α-immunopositive cells (Fig. 6d).

Discussion

DA is the predominant catecholamine neurotransmitter in the CNS. Disruptions of DA signaling contribute to various psychiatric and neurological disorders, including drug addiction, schizophrenia, and Parkinson's disease (Self and Nestler 1995; Hyman 1996). Extracellular DA levels are primarily regulated by DAT, an integral membrane protein that is a member of the Na^+/Cl^--dependent co-transporter gene family (Amara and Kuhar 1993). By removing extracellular DA and recycling it back to the neuron, DAT plays an essential role in terminating DA signaling. Pharmacological blockage of DAT by psychostimulants inhibits the reuptake of DA from the extracellular space, resulting in increased extracellular DA levels and augmented receptor stimulation (Horn 1990). Although pharmacological and genetic ablation (Grace 1995; Jones *et al.* 1998) studies indicate a critical role for DAT in the maintenance of DA neuronal homeostasis, the endogenous mechanisms regulating DAT expression and activity are poorly understood.

The PC12 cell line is derived from the rat pheochromocytoma. It is often used as an *in vitro* model to understand the physiology of central DA neurons (Roda *et al.* 1980; Tischler 2002; Fornai *et al.* 2007). A number of factors contribute to the wide use of PC12 cells: they are inexpensive as well as easy to handle, and mimic many features of central DA neurons. In fact, PC12 cells produce catecholamines (Markey *et al.* 1980; Roda *et al.* 1980; Vaccaro *et al.* 1980). In particular, they contain DA (Greene and Rein 1978) as the main catecholamine and bear DA receptors on their external membrane (Sampath *et al.* 1994). In light of the presence of DA and DA receptors, as well as DA uptake mechanisms, PC12 cell lines are considered to be closer to DA terminals than their ancestors (i.e. chromaffin cells of the adrenal medulla). This concept is reinforced by the presence of monoamine oxidase type A, which also characterizes DA neurons (Finberg and Youdim 1983), in contrast with the established prevalence of monoamine oxidase type B within chromaffin cells of the adrenal medulla (Youdim 1991).

Recently, we have demonstrated that TNF-α and its inducer play a neuroprotective role in the behavioral sensitization to and rewarding effects of METH by activating plasmalemmal and vesicular DAT as well as by inhibiting the METH-induced increase in extracellular DA levels (Nakajima *et al.* 2004; Niwa *et al.* 2007c,e). TNF-α modulates cellular responses through the ERK1/2 and NF-κB signaling pathways (van Vliet *et al.* 2005). The adaptor protein TNF receptor-associated factor 2 (TRAF2) and the serine and threonine protein kinase receptor-interacting protein are required for optimal TNF-induced signaling through ERK1/2, c-Jun N-termial kinase (JNK) and p38 mitogen-activated

Fig. 6 Involvement of TNF-α in shati-induced increase in DA uptake in PC12 cells. (a) TNF-α mRNA expression in PC12 cells transfected with the vector containing shati cDNA. The expression vector alone (pcDNA-DEST53), or the vector containing shati cDNA was introduced into PC12 cells. The cells were treated with 1 μM METH for 30 min. Values are means ± SE ($n = 8$). $^*p < 0.05$ versus mock-transfected group. $^\#p < 0.05$ versus METH + mock-transfected group. (b) Effect of shati-AS on TNF-α mRNA expression. Mice were administered METH (1 mg/kg, s.c.) for 5 days and decapitated 2 h after the final treatment. Values are means ± SE ($n = 8$–10). $^*p < 0.05$ versus corresponding saline-treated mice. $^\#p < 0.05$ versus saline + CSF and saline + shati-SC-treated mice. $^\$p < 0.05$ versus METH + CSF and METH + shati-SC-treated mice. (c) Involvement of TNF-α in shati-induced increase in [^{3}H] DA uptake in PC12 cells. The expression vector alone (pcDNA-DEST53), or the vector containing shati cDNA was introduced into PC12 cells. The cells were pre-treated with anti-TNF-α antibody (Ab; 50 ng/mL) or soluble TNF receptor I (sR I; 1 ng/mL) 10 min before their treatment with METH (1 μM, 30 min), and assayed for [^{3}H] DA uptake. The [^{3}H] DA uptake was 0.15 ± 0.02 pmol/10 min for the mock-transfected group. The final concentration of [^{3}H] DA was 20 nM. Values are means ± SE ($n = 10$). $^*p < 0.05$ versus mock-transfected group. $^\#p < 0.05$ versus the vector containing shati cDNA-transfected group. $^\$p < 0.05$ versus METH + mock-transfected group. $^+p < 0.05$ versus METH + the vector containing shati cDNA-transfected group. (d) Immunostaining of shati and TNF-α in PC12 cells transfected with the vector containing shati cDNA. The expression vector alone (pcDNA-DEST53) (i), or the vector containing shati cDNA (ii) (iii) was introduced into PC12 cells. The GFP or shati-immunopositive cells (green) were co-localized with TNF-α-immunopositive cells (red) (ii) (iii). Double immunostaining for GFP or S-4 and TNF-α in PC12 cells transfected with the vector containing shati cDNA reveals expression of shati in TNF-α-immunopositive cells (ii) (iii). Scale bar: 20 μm.

protein kinase (p38) (Baud and Karin 2001; Devin *et al.* 2003). MEK inhibitor PD98059 significantly decreases phosphorylated ERK1/2 without affecting total ERK level, MEK-JNK, -p38, and -NF-κB, resulting in loss of DAT surface expression and DAT capacity. According these results, MEK-ERK pathway, but not MEK-JNK, -p38, or -NF-κB pathway, is important for intracellular trafficking and transport capacity of DAT (Morón *et al.* 2003). Therefore, we investigated the involvement of TNF-α in DA uptake and the METH-induced inhibition of DA uptake in PC12 cells. Moreover, we examined the involvement of MEK-ERK signaling in the effects of TNF on DA uptake. TNF-α increased DA uptake via the MEK-ERK signaling pathway in PC12 cells (Figs 1 and 2). The increase was antagonized by the anti-TNF-α antibody and soluble TNF receptor I (Fig. 1b and c), suggesting that TNF-α certainly increases DA uptake in PC12 cells. Moreover, TNF-α inhibited the METH-induced decrease in DA uptake in PC12 cells (Fig. 3b). We have previously reported that the kinetics of [^{3}H] DA uptake in the absence or presence of TNF-α (10 ng/mL). Lineweaver-burk plots show that TNF-α potentiates [^{3}H] DA uptake by increasing the affinity (Km) accompanied by reducing the maximum number of [^{3}H] DATs (Vmax) (Nakajima *et al.* 2004). We suggest that TNF-α modulates the function of DAT, although it also regulates the expression of DAT. The expression of TNF-α is induced through the activation of transcription factors such as activator protein-1 (AP-1) and NF-κB by the activation of JNK/p38 (Guha *et al.* 2000; Rahman and MacNee 2000). Further, TNF-α acts on mitochondria to generate reactive oxygen species, which are involved in the activation of AP-1 and NF-κB (Rahman and MacNee 2000). Changes in transcription factors may result in long-term changes in gene expression, thereby contributing to neuronal adaptations that underlie behavioral sensitization (Nestler 2001). Therefore, we hypothesized that TNF-α inhibits the METH-induced increase in extracellular DA levels in the NAc by promoting DA uptake and finally inhibits METH-induced sensitization and rewarding effects (Nakajima *et al.* 2004; Niwa *et al.* 2007c,e).

'Shati', named after the symbol for Nagoya castle, was identified among molecules whose expression was regulated in the NAc of mice treated with METH (Niwa *et al.* 2007a). Recently, we have demonstrated that blockage of shati expression by shati-AS potentiates the increase in extracellular DA levels in the NAc and the decrease in synaptosomal and vesicular DA uptake in the midbrain induced by repeated METH treatment (Niwa *et al.* 2007a). Both TNF-α and shati increase DA uptake and inhibit the METH-induced decrease in DA uptake (Nakajima *et al.* 2004; Niwa *et al.* 2007a). Therefore, we investigated the precise mechanism of the effects of shati on DA uptake, and the METH-induced inhibition of DA uptake in PC12 cells. Moreover, we examined the relationship between shati and TNF-α in PC12 cells. Over-expression of shati by transfection of the vector containing shati cDNA (Fig. 4) dramatically induced the expression of shati mRNA (Fig. 5a) and TNF-α mRNA (Fig. 6a) in PC12 cells. No histological or mechanical disruption was produced by transfection of the vector (Fig. 4a). Over-expression of shati (Fig. 5a), which occurs in TNF-α-immunopositive cells (Fig. 6d), potentiated DA uptake and inhibited the METH-induced decrease in DA uptake (Fig. 5b) in PC12 cells by regulating TNF-α expression (Fig. 6a), since these effects were antagonized by anti-TNF-α antibody and soluble TNF receptor I used for the neutralization of TNF-α (Fig. 6c; Barone *et al.* 1997). These findings strongly suggest that the over-expression of shati elicited by METH serves as a homeostatic mechanism that prevents behavioral sensitization and rewarding effects by attenuating the METH-induced increase in extracellular DA

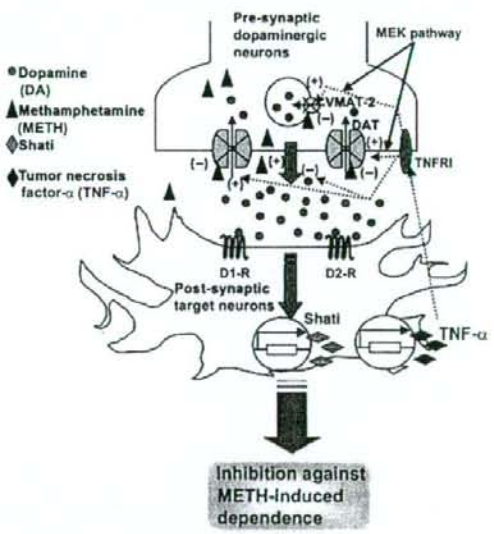

Fig. 7 Schema for regulation of TNF-α induced by shati on METH-induced DA responses. Under basal conditions, plasmalemmal DAT is involved in the reuptake of extracellular DA into the cytosol; subsequently the cytosolic DA is stored into synaptic vesicles via VMAT-2. Treatment of METH inhibits DA uptake through DA transporter and facilitates DA's release from pre-synaptic nerve terminals. METH is associated with an increase in extracellular DA levels in the brain, resulting in potentiation of the METH-induced dependence. METH induces shati and TNF-α expression in target neurons through the activation of DA receptors. TNF-α regulated by shati inhibits the METH-induced increase in extracellular DA levels in the nucleus accumbens by promoting DA uptake via MEK pathway and finally inhibits sensitization to and the rewarding effects of METH. DA: dopamine, METH: methamphetamine, TNF-α: tumor necrosis factor-α, D1-R: dopamine D1 receptor, D2-R: dopamine D2 receptor, DAT: dopamine transporter, VMAT-2: vesicular monoamine transporter-2, TNFR I: tumor necrosis factor type I receptor.

levels in the NAc through potentiation of plasmalemmal and vesicular DA uptake *via* induction of TNF-α expression (Fig. 7), although the mechanism by which TNF-α is regulated by shati remains to be elucidated.

Motif analyses have revealed that shati contains sequences of GNAT (Niwa *et al.* 2007a). Docking simulations with acetyl-CoA or ATP conducted using Molecular Operating Environment software reveal possible acetyl-CoA- and/or ATP-binding sites, since there is low potential energy for these interactions, in contrast with the prohibitively high energy of docking with DA, DNA or nuclear localization signals (Niwa *et al.* 2007a). These results suggest shati to have a physiological role in producing acetylcholine or the metabolic action of ATP. Accordingly, we have to investigate the mechanism by which shati regulates the production of acetylcholine or metabolic roles of ATP in subsequent studies.

In conclusion, we hypothesized that TNF-α expression induced by shati inhibits the METH-induced increase in extracellular DA levels in the NAc by promoting DA uptake and finally inhibits sensitization to and the rewarding effects of METH (Fig. 7). Targeting the shati-TNF-α system would provide a new therapeutic approach to the treatment of METH dependence.

Acknowledgments

This study was supported in part by Research Fellowships of the Japan Society for the Promotion of Science (JSPS) for Young Scientists; by Grants-in-aid for Scientific Research (B) and for Exploratory Research from the JSPS; by the 'Academic Frontier' Project for Private Universities (2007–2011) from the Ministry of Education, Culture, Sports, Science and Technology of Japan; by the International Research Project supported by the Meijo Asian Research Center (MARC); by Health and Labour Sciences Research on Regulatory Science of Pharmaceuticals and Medical Devices from the Ministry of Health, Labour and Welfare, Japan; by Research on Risk of Chemical Substances, Health and Labour Science Research Grants supported by the Ministry of Health, Labour and Welfare; by the Japan France Joint Health Research Program; and by the Uehara Foundation.

The authors are grateful to the Riken Cell Bank for the pheochromocytoma-12 (PC12) cells, and to Mrs. Nobuyoshi Hamada and Yoshiyuki Nakamura, Radioisotope Center Medical Branch, Nagoya University Graduate School of Medicine, for technical assistance.

References

Amara S. G. and Kuhar M. J. (1993) Neurotransmitter transporters: recent progress. *Annu. Rev. Neurosci.* **16**, 73–93.

Barone F. C., Arvin B., White R. F., Miller A., Webb C. L., Willette R. N., Lysko P. G. and Feuerstein G. Z. (1997) TNF-α. A mediator of focal ischemic brain injury. *Storoke* **28**, 1233–1244.

Baud V. and Karin K. (2001) Signal transduction by tumor necrosis factor and its relatives. *Trends Cell Biol.* **11**, 372–377. Review.

Boka G., Anglade P., Wallach D., Javoy-Agid F., Agid Y. and Hirsch E. C. (1994) Immunocytochemical analysis of tumor necrosis factor and its receptors in Parkinson's disease. *Neurosci. Lett.* **172**, 151–154.

Cen X., Nitta A., Ibi D., Zhao Y., Niwa M., Taguchi K., Hamada M., Ito Y., Ito Y., Wang L. and Nabeshima T. (2008) Identification of piccolo as a regulator of behavioral plasticity and dopamine transporter internalization. *Mol. Psychiatr.* **13**, 451–463.

Chen N. H., Reith M. E. and Quick M. W. (2004) Synaptic uptake and beyond: the sodium- and chloride-dependent neurotransmitter transporter family SLC6. *Pflugers Arch.* **447**, 519–531. Review.

Devin A., Lin Y. and Liu Z. G. (2003) The role of the death-domain kinase RIP in tumour-necrosis-factor-induced activation of mitogen-activated protein kinases. *EMBO* **4**, 623–627.

Finberg J. P. and Youdim M. B. (1983) Selective MAO A and B inhibitors: their mechanism of action and pharmacology. *Neuropharmacology* **22**, 441–446. Review.

Fog J. U., Khoshbouei H., Holy M. *et al.* (2006) Calmodulin kinase II interacts with the dopamine transporter C terminus to regulate amphetamine-induced reverse transport. *Neuron* **51**, 417–429.

Fornai F., Lenzi P., Lazzeri G., Ferrucci M., Fulceri F., Giorgi F. S., Falleni A., Ruggieri S. and Paparelli A. (2007) Fine ultrastructure and biochemistry of PC12 cells: a comparative approach to understand neurotoxicity. *Brain Res.* **1129**, 174–190.

Franklin K. B. J. and Paxinos G. (1997) *The Mouse Brain: In Stereotaxic Coordinates*. Academic Press, San Diego.

Grace A. A. (1995) The tonic/phasic model of dopamine system regulation: its relevance for understanding how stimulant abuse can alter basal ganglia function. *Drug Alcohol Depend.* **37**, 111–129. Review.

Greene L. A. and Rein G. (1978) Short-term regulation of catecholamine biosynthesis in a nerve growth factor responsive clonal line of rat pheochromocytoma cells. *J. Neurochem.* **30**, 549–555.

Guha M., Bai W., Nadler J. L. and Natarajan R. (2000) Molecular mechanisms of tumor necrosis factor α gene expression in monocytic cells via hyperglycemia-induced oxidant stress-dependent and -independent pathways. *J. Biol. Chem.* **275**, 17728–17739.

Horn A. S. (1990) Dopamine uptake: a review of progress in the last decade. *Prog. Neurobiol.* **34**, 387–400. review.

Hsu H., Xiong J. and Goeddel D. V. (1995) The TNF receptor 1-associated protein TRADD signals cell death and NF-kappa B activation. *Cell* **81**, 495–504.

Hyman S. E. (1996) Addiction to cocaine and amphetamine. *Neuron* **16**, 901–904.

Jones S. R., Gainetdinov R. R., Jaber M., Giros B., Wightman R. M. and Caron M. G. (1998) Profound neuronal plasticity in response to inactivation of the dopamine transporter. *Proc. Natl Acad. Sci. USA* **95**, 4029–4034.

Koob G. F. (1992) Drugs of abuse: anatomy, pharmacology and function of reward pathways. *Trends Pharmacol. Sci.* **13**, 177–184.

Koob G. F., Sanna P. P. and Bloom F. E. (1998) Neuroscience of addiction. *Neuron* **21**, 467–476.

Loder M. K. and Melikian H. E. (2003) The dopamine transporter constitutively internalizes and recycles in a protein kinase C-regulated manner in stably transfected PC12 cell lines. *J. Biol. Chem.* **278**, 22168–22174.

Maier S. F. and Watkins L. R. (1998) Cytokines for psychologists: implications of bidirectional immune-to-brain communication for understanding behavior, mood, and cognition. *Psychol. Rev.* **105**, 83–107.

Markey K. A., Kondo H., Shenkman L. and Goldstein M. (1980) Purification and characterization of tyrosine hydroxylase from a clonal pheochromocytoma cell line. *Mol. Pharmacol.* **17**, 79–85.

Melikian H. E. and Buckley K. M. (1999) Membrane trafficking regulates the activity of the human dopamine transporter. *J. Neurosci.* **19**, 7699–7710.

Morón J. A., Zakharova I., Ferrer J. V. *et al.* (2003) Mitogen-activated protein kinase regulates dopamine transporter surface expression and dopamine transport capacity. *J. Neurosci.* **23**, 8480–8488.

Nakajima A., Yamada K., Nagai T. *et al.* (2004) Role of tumor necrosis factor-α in methamphetamine-induced drug dependence and neurotoxicity. *J. Neurosci.* **24**, 2212–2225.

Nestler E. J. (2001) Molecular basis of long-term plasticity underlying addiction. *Nat. Rev. Neurosci.* **2**, 119–128.

Niwa M., Nitta A., Mizoguchi H., Ito Y., Noda Y., Nagai T. and Nabeshima T. (2007a) A novel molecule 'shati' is involved in methamphetamine-induced hyperlocomotion, sensitization, and conditioned place preference. *J. Neurosci.* **27**, 7604–7615.

Niwa M., Nitta A., Shen L., Noda Y. and Nabeshima T. (2007b) Involvement of glial cell line-derived neurotrophic factor in inhibitory effects of a hydrophobic dipeptide Leu-Ile on morphine-induced sensitization and rewarding effects. *Behav. Brain Res.* **179**, 167–171.

Niwa M., Nitta A., Yamada K. and Nabeshima T. (2007c) The roles of glial cell line-derived neurotrophic factor, tumor necrosis factor-α, and an inducer of these factors in drug dependence. *J. Pharmacol. Sci.* **104**, 116–121.

Niwa M., Nitta A., Yamada Y., Nakajima A., Saito K., Seishima M., Noda Y. and Nabeshima T. (2007d) Tumor necrosis factor-α and its inducer inhibit morphine-induced rewarding effects and sensitization. *Biol. Psychiatry* **62**, 658–668.

Niwa M., Nitta A., Yamada Y., Nakajima A., Saito K., Seishima M., Shen L., Noda Y., Furukawa S. and Nabeshima T. (2007e) An inducer for glial cell line-derived neurotrophic factor and tumor necrosis factor-α protects against methamphetamine-induced rewarding effects and sensitization. *Biol. Psychiatry* **61**, 890–901.

Niwa M., Yan Y. and Nabeshima T. (2008) Genes and molecules that can potentiate or attenuate psychostimulant dependence: relevance of data from animal models to human addiction. *Ann. NY Acad. Sci.* **1141**, 76–95.

Rahman I. and MacNee W. (2000) Regulation of redox glutathione levels and gene transcription in lung inflammation: therapeutic approaches. *Free Radic. Biol. Med.* **28**, 1405–1420.

Rawson R. A., Gonzales R. and Brethen P. (2002) Treatment of methamphetamine use disorders: an update. *J. Subst. Abuse Treat.* **23**, 145–150. Review.

Roda L. G., Nolan J. A., Kim S. U. and Hogue-Angeletti R. A. (1980) Isolation and characterization of chromaffin granules from a pheochromocytoma (PC 12) cell line. *Exp. Cell Res.* **128**, 103–109.

Sampath D., Jackson G. R., Werrbach-Perez K. and Perez-Polo J. R. (1994) Effects of nerve growth factor on glutathione peroxidase and catalase in PC12 cells. *J. Neurochem.* **62**, 2476–2479.

Self D. W. and Nestler E. J. (1995) Molecular mechanisms of drug reinforcement and addiction. *Annu. Rev. Neurosci.* **18**, 463–495. Review.

Sulzer D., Sonders M. S., Poulsen N. W. and Galli A. (2005) Mechanisms of neurotransmitter release by amphetamines: a review. *Prog. Neurobiol.* **75**, 406–433.

Tischler A. S. (2002) Chromaffin cells as models of endocrine cells and neurons. *Ann. NY Acad. Sci.* **971**, 366–370. Review.

Torres G. E., Gainetdinov R. R. and Caron M. G. (2003) Plasma membrane monoamine transporters: structure, regulation and function. *Nat. Rev. Neurosci.* **4**, 13–25. Review.

Vaccaro K. K., Liang B. T., Perelle B. A. and Perlman R. L. (1980) Tyrosine 3-monooxygenase regulates catecholamine synthesis in pheochromocytoma cells. *J. Biol. Chem.* **255**, 6539–6541.

Vassalli P. (1992) The pathophysiology of tumor necrosis factors. *Annu. Rev. Immunol.* **10**, 411–452. Review.

van Vliet C., Bukczynska P. E., Puryer M. A., Sadek C. M., Shields B. J., Tremblay M. L. and Tiganis T. (2005) Selective regulation of tumor necrosis factor-induced Erk signaling by Src family kinases and the T cell protein tyrosine phosphatase. *Nat. Immunol.* **6**, 253–260.

Wada R., Tifft C. J. and Proia R. L. (2000) Microglial activation precedes acute neurodegeneration in Sandhoff disease and is suppressed by bone marrow transplantation. *Proc. Natl Acad. Sci. USA* **97**, 10954–10959.

Wise R. A. (1996) Neurobiology of addiction. *Curr. Opin. Neurobiol.* **6**, 243–251.

Youdim M. B. (1991) PC12 cells as a window for the differentiation of neural crest into adrenergic nerve ending and adrenal medulla. *J. Neural Transm. Suppl.* **34**, 61–67.

ELSEVIER

Journal of Neuroimmunology 194 (2008) 54–61

Journal of
Neuroimmunology

www.elsevier.com/locate/jneuroim

Production and functions of IL-17 in microglia

Jun Kawanokuchi [a], Kouki Shimizu [a], Atsumi Nitta [b], Kiyofumi Yamada [b], Tetsuya Mizuno [a], Hideyuki Takeuchi [a], Akio Suzumura [a,*]

[*] *Department of Neuroimmunology, Research Institute of Environmental Medicine, Nagoya University, Furo-cho, Chikusaku, Nagoya 464-8601, Japan*
[b] *Department of Neuropsychopharmacology and Hospital Pharmacy, Nagoya University Graduate School of Medicine Showa-ku, Nagoya 466-8560, Japan*

Received 26 July 2007; received in revised form 16 November 2007; accepted 19 November 2007

Abstract

Interleukin (IL)-17-producing helper T cells may play a pivotal role in the pathogenesis of multiple sclerosis. Here, we examined the effects of IL-17 on microglia, which are known to be critically involved in multiple sclerosis. Treatment with IL-17 upregulated the microglial production of IL-6, macrophage inflammatory protein-2, nitric oxide, adhesion molecules, and neurotrophic factors. We also found that IL-17 was produced by microglia in response to IL-23 or IL-1β. Because microglia produce IL-1β and IL-23, these cytokines may act in an autocrine manner to induce IL-17 expression in microglia, and thereby contribute to autoimmune diseases, such as MS, in the central nervous system.

Keywords: Cytokine; IL-17; EAE; MS; Microglia

1. Introduction

Multiple sclerosis (MS) is a chronic inflammatory demyelinating disorder that affects the central nervous system (CNS). Although the etiology of MS is not fully understood, T helper 1 (Th1) cells and the cytokines that they produce are thought to play a role in the development of MS. Recently, interleukin (IL)-17 producing helper T (Th17) cells play important roles in the induction of autoimmune diseases including MS and the corresponding animal model—experimental autoimmune encephalomyelitis (EAE) (Hofstetter et al., 2005, Ishizu et al., 2005, Iwakura and Ishigame, 2006). It has been shown that IL-17 mRNA levels are high in both the cerebrospinal fluid and plaques of MS patients (Matusevicius et al., 1999, Lock et al., 2003). IL-17 is a T cell-derived proinflammatory molecule that stimulates epithelial, endothelial, and fibroblastic cells to produce other inflammatory cytokines and chemokines, including IL-6, macrophage inflammatory protein (MIP)-2, granulocyte-colony stimulating factor (G-CSF), and monocyte chemoattractant protein (MCP)-1 (Aggarwal and Gurney, 2002; Yao et al., 1995; Kennedy et al., 1996; Fossiez et al., 1996; Linden et al., 2000; Cai et al., 1998; Jovanovic et al., 1998; Laan et al., 1999). IL-17 also synergizes with other cytokines such as tumor necrosis factor (TNF)α and IL-1β to further induce chemokine expression (Jovanovic et al., 1998; Chabaud et al., 1998). Although the precise mechanisms that control Th17 cell development have yet to be elucidated, Th17 cells are thought to develop from naïve T helper (Th0) cells via a pathway that is different than the pathways that lead to the development of Th1 and Th2 cells. In the absence of interferon (IFN)γ and IL-4, IL-23 has been shown to maintaining Th17 phenotype in a manner that is not dependent on the transcription factors STAT1, T-bet, STAT4, and STAT6 (Aggarwal et al., 2003; Harrington et al., 2005; Park et al., 2005; Bettelli et al., 2006). Interestingly, a recent study revealed that IL-27 is a critical regulator of IL-17 production. IL-27 receptor-deficient mice were found to generate more IL-17-producing T helper cells and were hypersusceptible to EAE, suggesting that IL-27 negatively regulates the development of Th17 cells (Batten et al., 2006).

* Corresponding author. Department of Neuroimmunology, Research Institute of Environmental Medicine, Nagoya University, Furo-cho, Chikusaku, Nagoya 464-8601, Japan. Tel.: +81 52 789 3881; fax: +81 52 789 3885.
E-mail address: suzumura@riem.nagoya-u.ac.jp (A. Suzumura).

0165-5728/$ - see front matter © 2007 Elsevier B.V. All rights reserved.
doi:10.1016/j.jneuroim.2007.11.006

IL-17 levels have been shown to be significantly higher in the cerebrospinal fluid of patients with active optico-spinal MS (Ishizu et al., 2005) and in the CNS of EAE mice (Hofstetter et al., 2005). The effects of IL-17 on CNS cells, however, are unclear. In order to uncover the contribution of IL-17 to inflammatory demyelination in the CNS, we have examined the effects of IL-17 on microglia, which function as antigen-presenting cells and effector cells in the CNS during inflammatory demyelination.

2. Materials and methods

2.1. Reagents

Lipopolysaccharide (LPS), human recombinant transforming growth factor (TGF)-β, and mouse recombinant IL-17 and IL-23 were obtained from Sigma-Aldrich (St. Louis, MO, USA). Mouse recombinant IL-1β, TNFα, and IFNγ were purchased from Techne (Minneapolis, MN, USA). Sulfonylamide, *N*-(1-naphthyl)ethylenediamine, and phosphate for Griess reagent (Ignarro et al., 1987) were also purchased from Sigma-Aldrich.

2.2. Cell culture

The protocols for the animal experiments were approved by the Animal Experiment Committee of Nagoya University. All primary cultures were prepared from C57BL/6J mice (Japan SLC, Hamamatsu, Shizuoka, Japan). Microglia were isolated from primary mixed glial cell cultures prepared from newborn mice on day 14 using the "shaking off" method as previously described (Suzumura et al., 1987); the purity of the cultures was almost 100%, as determined by immunostaining with anti-CD11b antibodies. The cultures were maintained in Dulbecco's modified Eagle's minimum essential medium (Sigma-Aldrich) supplemented with 10% fetal calf serum (JRH Biosciences, Lenexa, KS, USA), 5 μg/ml bovine insulin (Sigma), and 0.2% glucose.

Astrocyte-enriched cultures were prepared as described previously (Kuno et al., 2006). Briefly, the mixed glial cell cultures were trypsinized after the microglia were collected, and replated in Petri dishes. After this procedure was repeated three times, the cultures that had undergone four passages were used as the astrocyte-enriched cultures. The purity of the cultures were more than 80% as determined by immunostaining with anti-glial fibrillary acidic protein (GFAP). Peritoneal macrophages were collected from mice intraperitoneally injected with thioglycolate 48 h prior to collection. T cell-rich lymphocytes were separated from mouse spleens. Neuronal cultures were prepared from mice at embryonic day 17 as described previously (Takeuchi et al., 2005). Briefly, cortices were dissected and freed of meninges. Cortical fragments were dissociated into single cells using dissociation solution, and they were resuspended in Nerve-Cell Culture Medium (serum-free conditioned medium from 48-h rat astrocyte confluent cultures based on Dulbecco's modified Eagle's minimum essential medium/F-12 with N2 supplement, Sumitomo Bakelite, Akita, Japan). The purity of the cultures was more than 95% as determined by NeuN-specific immunostaining.

2.3. Expression of IL-17 receptors

The mRNA expression of the IL-17 receptor was examined using reverse transcription-polymerase chain reactions (RT-PCRs). Microglia, astrocytes, or neurons were cultured for 3 days before total cellular RNA was extracted using an RNase Mini Kit (Qiagen). cDNA encoding the IL-17 receptor was examined by RT-PCR analysis using SuperScript II (Invitrogen), AmpliTaq DNA polymerase (Applied Biosystems), and the specific primers shown in Table 1. Amplification within the linear range using 5 μl of each cDNA sample was achieved following 30 cycles in a DNA thermal cycler under conditions that were optimized for each set of primers.

The protein level of IL-17 receptor expression was examined using Western blot analysis. Samples (20 μg/well) were electrophoresed on 7.5% SDS-polyacrylamide gels (Invitrogen) according to the Laemmli method (Laemmli and Favre, 1973). After electrophoresis, proteins were transferred from the gels to nitrocellulose membranes (Amersham Bioscience, Buckinghamshire, UK) using standard procedures (Towbin et al., 1979). Nonspecific binding was blocked with 5% nonfat dry milk in TBST buffer (5 mM Tris–HCl, pH 7.6, 136 mM NaCl, 0.05% Tween 20) for 1 h. Blots were incubated for 12 h at 4 °C with rat anti-mouse IL-17 receptor antibody (R&D Systems) (1:1000 dilution). Blots were washed four times in TBST: the first time for 20 min and 10 min each time thereafter. We then incubated the washed blots for 1 h at room temperature with a

Table 1
Primer sequences used for RT-PCR analysis

GAPDH sense, 5′-ACTCACGGGAAATTCAACG
GAPDH antisense, 5′-CCCTGTTGCTGTAGCCGTA
IL-17R sense, 5′-CTAAACTGCACGGTCAAGAAT
IL-17R antisense, 5′-ATGAACCAGTACACCCAC
TNFα sense 5′-ATGAGCACAGAAAGCATGATCCGC
TNFα antisense 5′-CCAAAGTAGACCTGCCCGGACTC
IL-1β sense, 5′-ATGGCAACTGTTCCTGAACTCAACT
IL-1β antisense, 5′-CAGGACAGGTATAGATTCTTTCCTTT
IL-6 sense, 5′-ATGAAGTTCCTCTCTGCAAGAGACT
IL-6 antisense, 5′-CACTAGGTTTGCCGAGTAGGATCTC
MIP-2 sense, 5′-CCGGCTCCTCAGTGCTG
MIP-2 antisense, 5′-GGTCAGTTAGCCTTGCCTTT
IL-17 sense, 5′-CAGGACGCGCAAAACATGA
IL-17 antisense, 5′-GCAACAGCATCAGAGAGACACAGAT
iNOS sense, 5′-CCCTTCCGAAGTTTCTGGCAGCAGC
iNOS antisense, 5′-GGCTGTCAGAGCCTCGTGGCTTTGG
NGF sense, 5′-CATAGCGTAATGTCCATGTTGTTCT
NGF antisense, 5′-CTTCTCATCTGTTGTCAACGC
BDNF sense, 5′-AGCCTCCTCTGCTCTTTCTG
BDNF antisense, 5′-TTGTCTATGCCCCTGCAGCC
GDNF sense, 5′-ATTTTATTCAAGGCCACCATTA
GDNF antisense, 5′-GATACATCCACACCGTTTTAGC
MHC class II antigen sense, 5′-AAGAAGGAGACTGTCTGGATGC
MHC class II antigen antisense, 5′-TGAATGATGAAGATGGTGCCC
ICAM-1 sense, 5′-TTCACACTGAATGCCAGCTC
ICAM-1 antisense, 5′-GTCTGCTGAGACCCCTCTTG
VCAM-1 sense, 5′-ATTTTCTGGGGCAGGAAGTT
VCAM-1 antisense, 5′-ACGTCAGAACAACCGAATCC

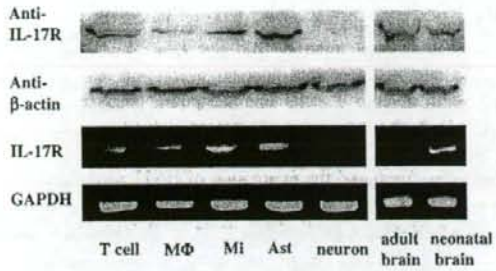

Fig. 1. Expression of IL-17 receptor mRNA and protein in neural cells. Microglia and astrocytes along with splenic T cells and macrophages express IL-17 receptor mRNA and protein, whereas neurons do not. MΦ, macrophages; Mi, microglia; Ast, astrocytes (left panel). The mRNA expression of IL-17 receptor in adult brain was lower than that of neonatal, but protein level of IL-17 receptor was the same as neonatal (right panel).

1:5000 dilution of peroxidase-conjugated, anti-rat IgG secondary antibody (Amersham Bioscience) followed by an additional rinse. IL-17 receptor was detected by ECL (Amersham Bioscience). The molecular weight of IL-17 receptor was determined by running molecular weight markers (Invitrogen) in an adjacent lane. Spleen cells served as a positive control.

2.4. Effects of IL-17 on the production of cytokines, neurotrophic factors and NO by microglia

Microglia and astrocytes were cultured in 24-well plates at a concentration of 1×10^6 cells/ml with or without 1 μg/ml LPS for 24 to 72 h in presence of various doses of IL-17 (1–100 ng/ml). The supernatants were then collected and stored at −80 °C until they were assessed. Total cellular RNA was extracted from remaining cells using an RNase Mini Kit (Qiagen). cDNAs encoding mouse TNFα, IL-1β, IL-6, iNOS, MIP-2 (the functional analogue of human IL-8), Nerve growth factor (NGF), glial cell line-derived neurotrophic factor (GDNF), brain-derived neurotrophic factor (BDNF) and IL-17 were generated and amplified in RT-PCRs as described above using the specific primers shown in Table 1.

Cytokine production was measured using ELISA kits specific for TNFα, IL-6 (Techne), MIP-2, and IL-17 (R&D).

Cellular levels of NGF and BDNF in the microglia were also assessed as follows: stimulated microglial cultures were washed four times in cold PBS, the cells were lysed using sonication in ice-cold PBS containing protease inhibitors (complete mini EDTA-free; Roche, Mannheim, Germany), and the lysates were assayed for cellular NGF and BDNF using ELISA kits specific for NGF and BDNF (Promega, WI, USA). Cytoplasmic GDNF content was measured by an enzyme immunoassay (EIA) as described (Nitta et al., 1999). The EIA system for GDNF was based on the method originally developed for the EIA of NGF, BDNF, and NT-3 (Furukawa et al., 1983; Kaechi et al., 1993; Nitta et al., 1999; Nitta et al., 2004). Antibodies against GDNF were produced by immunizing rabbits with purified human recombinant GDNF. GDNF protein (0.5 mg) in phosphate-buffered saline (PBS; 5 ml) was emulsified with an equal volume of Freund's adjuvant and injected intradermally into rabbits four times at 2-week intervals. Animals were exsanguinated 1 week after the final injection. To affinity purify the antibody, antiserum (1 ml) first was loaded onto a GDNF-linked column (1-ml bed volume; Affi-Gel 10; Bio-Rad, Hercules, CA). After extensive sequential washing with three buffers, 0.1 M Tris–HCl (pH 7.4) containing 0.9% NaCl, 0.05 M borate buffer (pH 8.0), and 0.05 mM sodium acetate buffer (pH 5.0), the bound antibodies were eluted with a 0.1 M glycine–HCl buffer (pH 2.0). A part of the purified anti-GDNF antibody preparation was eluted and biotinylated. The detection limit of the EIAs was as low as 1 pg/ml.

NO production was determined using the Griess reaction as described (Pollock et al., 1991). Briefly, 50-μl aliquots of the supernatants were mixed with an equal volume of Griess reagent (0.1% *N*-ethylenediamine dihydrochloride, 1% sulfanilamide, and 2.5% phosphoric acid) and incubated for 5 min at room temperature. The absorbance at 540 nm was measured

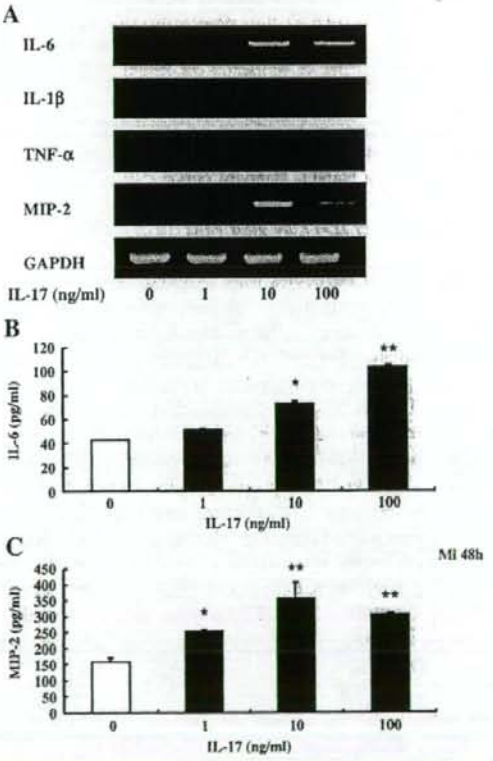

Fig. 2. The effects of IL-17 on cytokine production by microglia. Microglia were treated with IL-17 for 48 h. (A) At concentrations greater than 1 ng/ml, IL-17 induced the expression of IL-6 and MIP-2 mRNA. Similar results were obtained for IL-6 (B) and MIP-2 (C) protein using specific ELISAs. The values shown are the means±S.D. $^*P<0.05$ and $^{**}P<0.01$ compared with untreated microglia. The data represent typical samples performed in triplicate in three independent experiments.

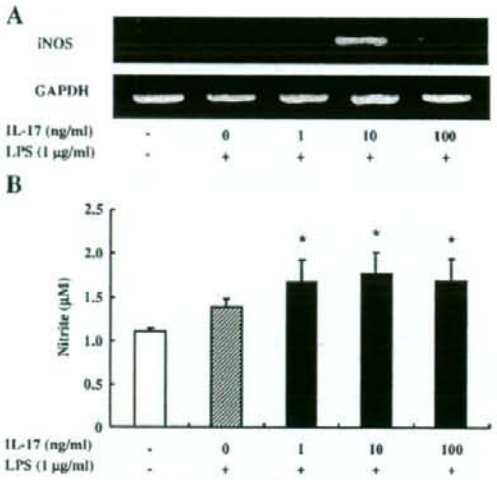

Fig. 3. The effects of IL-17 on NO production and iNOS expression in LPS-stimulated microglia. Microglia were stimulated with LPS for 48 h in the presence of various concentrations of IL-17. IL-17 enhanced iNOS mRNA expression (A) and NO production (B). The values shown are the means±S.D. $^{*}P<0.05$ compared with LPS-stimulated microglia in the absence of IL-17. The data represent typical samples performed in triplicate in three independent experiments.

using a microtiter plate reader. Nitrite concentrations were calculated from a $NaNO_2$ standard curve.

2.5. Production of IL-17 by glial cells

Microglia and astrocytes were cultured for 72 h in 6-well plates at a concentration of 1×10^6 cells/ml with various doses of IL-23 (1–100 ng/ml). The culture supernatants were then collected and stored at −80°C until they were assessed. IL-17 production was measured using an ELISA kit specific for murine IL-17 (R&D). Total cellular RNA was extracted from the remaining cells using an RNase Mini Kit (Qiagen). cDNAs encoding mouse IL-17 were amplified using RT-PCRs as described above and the specific primers shown in Table 1. In some experiments, cytoplasmic levels of IL-17 in the microglia were also assessed as follows: stimulated microglial cultures were washed four times in cold PBS, the cells were lysed using sonication in ice-cold PBS containing protease inhibitors (complete mini EDTA-free; Roche, Mannheim, Germany), and the lysates were assayed for cellular IL-17 using ELISAs.

3. Results

3.1. Expression of the IL-17 receptor

Increased levels of IL-17 have been observed in the cerebrospinal fluid from patients with active MS as well as in the CNS of EAE mice. Thus, we assessed the expression of IL-17 receptor in CNS cells. RT-PCR demonstrated that neonatal microglia and astrocytes along with splenic T cells and peripheral macrophages expressed IL-17 receptor mRNA, whereas embryonic neurons did not (Fig. 1). Western blot analysis demonstrated that neonatal microglia and astrocytes along with splenic T cells and peripheral macrophages expressed IL-17 receptor protein, whereas embryonic neurons did not (Fig. 1).

We next compared the expression of IL-17 receptor mRNA and protein in adult brain with that of neonatal brain. The expression of mRNA for IL-17 receptor in adult brain was lower than that of neonatal, but protein level of IL-17 receptor was almost identical in these 2 samples (Fig. 1, left panel).

3.2. Effects of IL-17 on microglia

We then assessed the effects of IL-17 on microglia. IL-17 induced the mRNA expression of the inflammatory cytokines IL-6 and MIP-2 with maximum induction observed at 10 ng/ml (Fig. 2A). IL-17, however, did not significantly induce the expression of mRNA encoding IL-1β or TNFα. Upregulation of the expression of IL-6 and MIP-2 protein by IL-17 was confirmed with ELISAs; IL-17 at a concentration of 10 ng/ml or greater significantly increased the production of IL-6 and MIP-2 by microglia (Fig. 2B), whereas IL-1β and TNFα were not detected in the supernatants (data not shown). Although IL-17 by itself did not induce the expression of iNOS mRNA and NO production in unstimulated microglia, it enhanced iNOS mRNA expression and NO production in LPS-stimulated microglia; the maximum increase was observed with 10 ng/ml IL-17 (Fig. 3). In addition, IL-17 dose-dependently upregulated the expression of neurotrophic factors NGF, BDNF, and GDNF (Figs. 4 and 5). IL-17 itself did not induce the expression of mRNA encoding class II major histocompatibility complex (MHC) antigen or cell adhesion molecules (data not shown). On the other hand, the expression of intercellular adhesion molecule (ICAM)-1 and vascular cell adhesion molecule (VCAM)-1 mRNA was upregulated in INFγ-stimulated microglia following treatment with IL-17, whereas it did not affect the expression of class II MHC antigen in these cells (Fig. 6). In contrast to the proinflammatory effects, IL-17 increased the expression of neurotrophic factors in microglia, which may contribute to anti-inflammatory defense mechanisms in the CNS and implies that microglia have multiple functions.

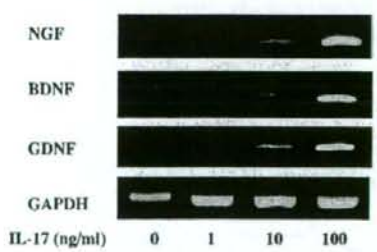

Fig. 4. The effects of IL-17 on the expression of mRNA coding for neurotrophic factors in microglia. Microglia were treated with IL-17 for 72 h. IL-17 dose-dependently induced the expression of NGF, BDNF, and GDNF mRNA.

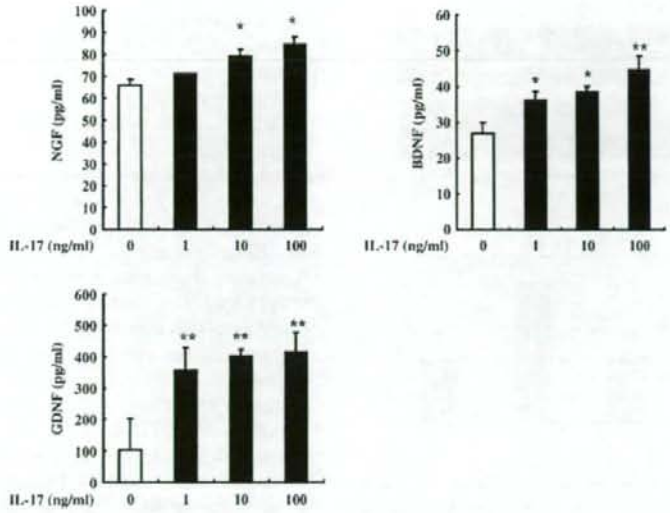

Fig. 5. The effects of IL-17 on the expression of neurotrophic factors in microglia. Microglia were treated with IL-17 for 72 h. IL-17 dose-dependently induced the expression of NGF, BDNF, and GDNF. The values shown are the means ± S.D. *$P<0.05$ and **$P<0.01$ compared with untreated microglia. The data represent typical samples performed in triplicate in three independent experiments.

3.3. Production of IL-17 by microglia

IL-17 is reported to be a T cell-specific cytokine (Yao et al., 1995). A study that analyzed human astrocytes using cDNA microarrays, however, suggested that CNS cells produce IL-17 (Meeuwsen et al., 2003). Thus, we assessed IL-17 production in glial cells. Although unstimulated microglia did not express mRNA coding for IL-17, IL-23 induced IL-17 mRNA expression in microglia in a dose-dependent manner. Because ELISAs failed to detect IL-17 in the supernatant of IL-23-stimulated microglia, we measured the cytoplasmic levels of IL-17 in IL-23-stimulated microglia. IL-23 (≥1 ng/ml) significantly increased the cytoplasmic level of IL-17 in a dose-dependent manner (Fig. 7). IL-1β (≥1 ng/ml) also induced the expression of IL-17 mRNA and increased the cytoplasmic level of IL-17 in microglia; maximum induction was observed at 10 ng/ml (Fig. 8). On the contrary, stimulation with IL-23 or IL-23 and IL-1β did not induce IL-17 mRNA expression in astrocytes (data not shown). In the presence of IL-6, TGF-β derived from regulatory T cells induces upregulation of IL-23 receptor expression in Th17 cells (Ivanov et al., 2006). Neither IL-6 nor TGF-β, however, enhanced IL-17

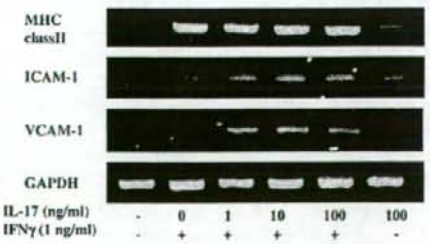

Fig. 6. The effects of IL-17 on the expression of mRNA encoding MHC antigen and adhesion molecules. Microglia were stimulated with IFNγ for 48 h in the presence of various concentrations of IL-17. IL-17 enhanced ICAM-1 and VCAM-1 mRNA expression in INFγ-stimulated microglia, whereas it did not affect MHC class II antigen mRNA levels in these cells.

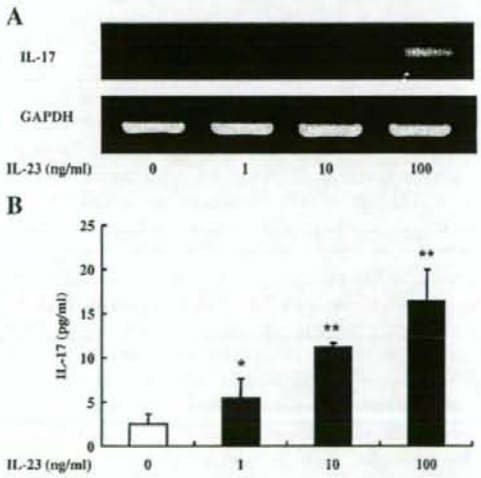

Fig. 7. IL-23 induces IL-17 production by microglia. Microglia were stimulated with various concentrations of IL-23 for 72 h. IL-23 dose-dependently induced IL-17 mRNA expression (A) and increased cytoplasmic IL-17 levels in microglia (B). The values shown are the means ± S.D. *$P<0.05$ and **$P<0.01$ compared with untreated microglia. The data represent typical samples performed in triplicate in three independent experiments.

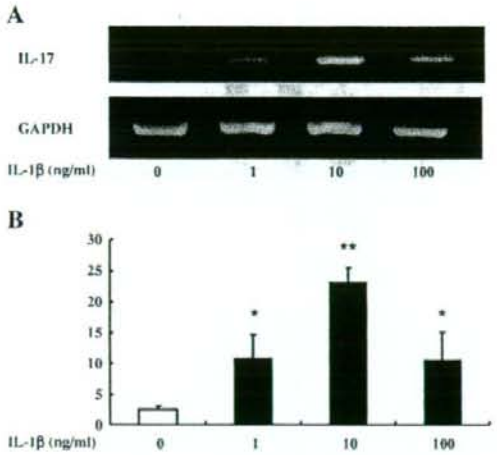

Fig. 8. IL-1β induces IL-17 production by microglia. Microglia were stimulated with various concentrations of IL-1β for 72 h. IL-1β induced IL-17 mRNA expression (A) and increased cytoplasmic IL-17 levels in microglia (B). The values shown are the means±S.D. *$P<0.05$ and **$P<0.01$ compared with untreated microglia. The data represent typical samples performed in triplicate in three independent experiments.

production in unstimulated microglia or in IL-23-stimulated microglia (data not shown). Stimulation with both IL-6 (100 ng/ml) and TGF-β (10 ng/ml) also failed to enhance the level of IL-17 produced by IL-23-stimulated microglia (data not shown).

4. Discussion

IL-17 has been associated with various autoimmune diseases, although its regulation and functional roles remain to be clarified. Antibodies specific for IL-17 reportedly inhibit chemokine expression in the brain during EAE, whereas overexpression of IL-17 in lung epithelia results in chemokine production and leukocyte infiltration. Thus, IL-17 expression characterizes a unique T helper lineage that regulates tissue inflammation (Park et al., 2005). Here we have evaluated the effects of IL-17 on neural cells *in vitro*. In the CNS, microglia and astrocytes express IL-17 receptors, whereas neurons do not. We then examined the effects of IL-17 on microglia—the antigen-presenting effector cells that can induce autoimmune inflammatory processes in the CNS. Because both IL-4 and IFNγ negatively regulate the production of IL-17 by T helper cells during the effector phase, Th17 cells may have roles that are distinct from those of Th1 and Th2 cells. The effects of IL-17 on microglia, however, are similar to those of Th1 cytokines; IL-17 enhanced inflammatory cytokine and chemokine production by microglia. IL-17 did not affect IFNγ-induced MHC class II antigen expression by microglia, whereas it increased the IFNγ-induced expression of adhesion molecules by these cells. IL-17 by itself did not induce iNOS expression or NO production, although it enhanced both of these phenomena in LPS-stimulated microglia. In rodent astrocytes, it has been shown that IL-17 enhances IFNγ-induced iNOS expression, which is suppressed by inhibitors of NF-κB or p38 MAP kinase (Trajkovic et al., 2001). Thus, IL-17 functions as a proinflammatory cytokine that works synergistically with other inflammatory stimuli in the CNS.

In addition to the proinflammatory effects on microglia, IL-17 also enhanced the expression of neurotrophic factors by microglia. We and other groups have previously shown that proinflammatory cytokines or inflammatory stimuli induce the expression of neurotrophic factors in microglia (Suzumura et al., 2006; Bessis et al., 2007). This may contribute to anti-inflammatory defense mechanisms in the CNS and implies that microglia may have multiple functions.

Previous cDNA microarray and immunohistochemical studies have suggested that astrocytes produce IL-17 (Meeuwsen et al., 2003; Li et al., 2005). In this study, we showed for the first time that microglia produce IL-17 in response to IL-23 or IL-1β. Although IL-1β and IL-23 induced IL-17 mRNA expression in microglia, we did not detect IL-17 in the supernatant of these cells. It is possible that IL-1β and IL-23 stimulate microglia to produce very low amount of IL-17 that cannot be detected with a commercially available ELISA kit, or that microglia may require another stimulatory signal before they release IL-17.

The same stimulus, however, did not induce the expression of IL-17 mRNA and protein in astrocytes. Thus, other stimuli may induce astrocytes to produce IL-17. Alternatively, this result may be due to differences between the species. As we and other groups have shown, IL-1β and IL-23 are produced by microglia in the CNS (Sonobe et al., 2005; Suzumura et al., 2006; Li et al., 2007). Therefore, it is possible that IL-1β and IL-23 may function as autocrine mediators that induce IL-17 expression by microglia.

Both Th1 and Th2 cytokines negatively regulate the differentiation of IL-17-producing T cells (Iwakura and Ishigame, 2006). In contrast, recent studies suggest that TGF-β derived from regulatory T cells induces an upregulation of IL-23 receptor expression and differentiation of Th17 cells in the presence of IL-6 (Ivanov et al., 2006; Valdhoen et al., 2006). Neither TGF-β nor IL-6, however, affects IL-17 production in microglia. Treatment of IL-23-stimulated microglia with both TGF-β and IL-6 also failed to enhance IL-17 production. These results suggest that different regulatory mechanisms control IL-17 production in microglia and Th17 cells.

Microglia play a pivotal role in the pathogenesis of inflammatory autoimmune diseases in the CNS. Thus, therapeutic targeting of the microglial production of IL-17 might be a useful strategy to treat MS. Because IL-17 deficiency has been demonstrated to ameliorate EAE in mice (Komiyama et al., 2006), induction of neutralizing antibodies that target the IL-23/IL-17 immune axis in microglia may provide a novel therapeutic approach for the treatment of MS. Indeed, targeting IL-23 with neutralizing antibodies ameliorates EAE and reduces serum levels of IL-17 (Chen et al., 2006). Moreover, a previous study demonstrated that blocking IL-17 with neutralizing antibodies induced by an active vaccination efficiently delays the onset of disease and reduces the severity of EAE (Röhn et al., 2006). Inflammatory autoimmune diseases such as MS, however, are chronic in nature, and treatment of these diseases with autoantibodies is extremely costly. Active

vaccination against IL-17 may therefore be an attractive therapeutic alternative, which could allow more patients access to an effective therapy that acts at an earlier stage of disease.

Acknowledgments

This work was supported in part by a Grant-in-Aid for Scientific Research and for the Creation of Innovations through the Business-Academic-Public Sector Cooperation from the Ministry of Education, Culture, Sports, Science and Technology of Japan as well as a Grant-in-Aid for Medical Frontier Strategy Research and for Research on Intractable Diseases from the Japanese Ministry of Health, Labour and Welfare. This work was also supported by the 21st COE Program "Integrated Molecular Medicine for Neuronal and Neoplastic Disorders" from the Ministry of Education, Culture, Sports, Science and Technology.

References

Aggarwal, S., Gurney, A.L., 2002. IL-17: prototype member of an emerging cytokine family. J. Leukoc. Biol. 71, 1–8.

Aggarwal, S., Ghilardi, N., Xie, M.H., de Sauvage, F.J., Gurney, A.L., 2003. Interleukin-23 promotes a distinct CD4 T cell activation state characterized by the production of interleukin-17. J. Biol. Chem. 278 (3), 1910–1914.

Batten, M., Li, J., Yi, S., Kljavin, N.M., Danilenko, D.M., Lucas, S., Lee, J., de Sauvage, F.J., Ghilardi, N., 2006. Interleukin 27 limits autoimmune encephalomyelitis by suppressing the development of interleukin 17-producing T cells. Nat. Immunol. 7, 929–936.

Bessis, A., Bechade, C., Bernard, D., Roumier, A., 2007. Microglial control of neuronal death and synaptic properties. Glia 55 (3), 233–238 Review.

Bettelli, E., Carrier, Y., Gao, W., Korn, T., Strom, T.B., Oukka, M., Weiner, H.L., Kuchroo, V.K., 2006. Reciprocal developmental pathways for the generation of pathogenic effector TH17 and regulatory T cells. Nature 441 (7090), 235–238.

Cai, X.Y., Gommoll Jr., C.P., Justice, L., Narula, S.K., Fine, J.S., 1998. Regulation of granulocyte colony-stimulating factor gene expression by interleukin-17. Immunol. Lett. 62, 51–58.

Chabaud, M., Fossiez, F., Taupin, J.L., Miossec, P., 1998. Enhancing effect of IL-17 on IL-1-induced IL-6 and leukemia inhibitory factor production by rheumatoid arthritis synoviocytes and its regulation by Th2 cytokines. J. Immunol. 161, 409–414.

Chen, Y., Langrish, C.L., McKenzie, B., Joyce-Shaikh, B., Stumbofer, J.S., McClanahan, T., Blumenschein, W., Churakovsa, T., Low, J., Presta, L., Hunter, C.A., Kastelein, R.A., Cua, D.J., 2006. Anti-IL-23 therapy inhibits multiple inflammatory pathways and ameliorates autoimmune encephalomyelitis. J. Clin. Invest. 116 (5), 1317–1326.

Fossiez, F., Djossou, O., Chomarat, P., Flores-Romo, L., Ait-Yahia, S., Maat, C., Pin, J.J., Garrone, P., Garcia, E., Saeland, S., Blanchard, D., Gaillard, C., Das, M.B., Rouvier, E., Golstein, P., Banchereau, J., Lebecque, S., 1996. T cell interleukin-17 induces stromal cells to produce proinflammatory and hematopoietic cytokines. J. Exp. Med. 183, 2593–2603.

Furukawa, S., Kamo, I., Furukawa, Y., Akazawa, S., Satoyoshi, E., Itoh, K., Hayashi, K., 1983. A highly sensitive enzyme immunoassay for mouse beta nerve growth factor. J. Neurochem. 40, 734–744.

Harrington, L.E., Hatton, R.D., Mangan, P.R., Turner, H., Murphy, T.L., Murphy, K.M., Weaver, C.T., 2005. Interleukin 17-producing $CD4^+$ effector T cells develop via a lineage distinct from the T helper type 1 and 2 lineages. Nat. Immunol. 6 (11), 1123–1132.

Hofstetter, H.H., Ibrahim, S.M., Koczan, D., Kruse, N., Weishaupt, A., Toyka, K.V., Gold, R., 2005. Therapeutic efficacy of IL-17 neutralization in murine experimental autoimmune encephalomyelitis. Cell Immunol. 237 (2), 123–130.

Ignarro, L.J., Buga, G.M., Wood, K.S., Byrns, R.E., Chaudhuri, G., 1987. Endothelium-derived relaxing factor produced and released from artery and vein in nitric oxide. Proc. Natl. Acad. Sci. USA, 84, 9265–9269.

Ishizu, T., Osoegawa, M., Mei, F.J., Kikuchi, H., Tanaka, M., Takakura, Y., Minohara, M., Murai, H., Mihara, F., Taniwaki, T., Kira, J., 2005. Intrathecal activation of the IL-17/IL-8 axis in opticospinal multiple sclerosis. Brain 128, 988–1002.

Ivanov, I.I., McKenzie, B.S., Zhou, L., Tadokoro, C., Lepelley, A., Lafaille, J., Cua, D., Littman, D., 2006. The orphan nuclear receptor RORgammat directs the differentiation program of proinflammatory $IL\text{-}17^+$ T helper cells. Cell 126, 1121–1133.

Iwakura, Y., Ishigame, H., 2006. The IL-23/IL-17 axis in inflammation. J. Clin. Invest. 116 (5), 1218–1922.

Jovanovic, D.V., Di, B.J.A., Martel-Pelletier, J., Jolicoeur, F.C., He, Y., Zhang, M., Mineau, F., Pelletier, J.P., 1998. IL-17 stimulates the production and expression of proinflammatory cytokines, IL-b and TNFa, by human macrophages. J. Immunol. 160, 3513–3521.

Kaechi, K., Furukawa, Y., Ikegami, R., Nakamura, N., Omae, F., Hashimoto, Y., Hayashi, K., Furukawa, S., 1993. Pharmacological induction of physiologically active nerve growth factor in rat peripheral nervous system. J. Pharmacol. Exp. Ther. 264, 321–326.

Kennedy, J., Rossi, D.L., Zurawski, S.M., Vega Jr., F., Kastelein, R.A., Wagner, J.L., Hannum, C.H., Zlotnik, A., 1996. Mouse IL-17: a cytokine preferentially expressed by alpha beta $TCR+CD4^-CD8^-$ T cells. J. Interferon Cytokine Res. 16, 611–617.

Komiyama, Y., Nakae, S., Matsuki, T., Nambu, A., Ishigame, H., Kakuta, S., Sudo, K., Iwakura, Y., 2006. IL-17 plays an important role in the development of experimental autoimmune encephalomyelitis. J. Immunol. 177, 566–573.

Kuno, R., Yoshida, Y., Nitta, A., Nabeshima, T., Wang, J., Sonobe, Y., Kawanokuchi, J., Takeuchi, H., Mizuno, T., Suzumura, A., 2006. The role of TNF-alpha and its receptors in the production of NGF and GDNF by astrocytes. Brain Res. 1116 (1), 12–18.

Laan, M., Cui, Z.H., Hoshino, H., Lotvall, J., Sjostrand, M., Gruenert, D.C., Skoogh, B.E., Linden, A., 1999. Neutrophil recruitment by human IL-17 via C–X–C chemokine release in the airways. J. Immunol. 162, 2347–2352.

Laemmli, U.K., Favre, M., 1973. Maturation of the head of bacteriophage T4. I. DNA packaging events. J. Mol. Biol. 80 (4), 575–579.

Li, G.Z., Zhong, D., Yang, L.M., Sun, B., Zhong, Z.H., Yin, Y.H., Cheng, J., Yan, B.B., Li, H.L., 2005. Expression of interleukin-17 in ischemic brain tissue. Scand. J. Immunol. 62 (5), 481–486.

Li, Y., Chu, N., Hu, A., Gran, B., Rostami, A., Zhang, G.X., 2007. Increased IL-23p19 expression in multiple sclerosis lesions and its induction in microglia. Brain 130 (Pt2), 490–501.

Linden, A., Hoshino, H., Laan, M., 2000. Airway neutrophils and interleukin-17. Eur. Respir. J. 15, 973–977.

Lock, C., Hermans, G., Pedotti, R., Brendolan, A., Schadt, E., Garren, H., Langer-Gould, A., Strober, S., Cannella, B., Allard, J., Klonowski, P., Austin, A., Lad, N., Kaminski, N., Galli, S.J., Oksenberg, J.R., Raine, C.S., Heller, R., Steinman, L., 2003. Gene-microarray analysis of multiple sclerosis lesions yields new targets validated in autoimmune encephalomyelitis. Nat. Med. 8 (5), 500–208.

Matusevicius, D., Kivisakk, P., He, B., Kostulas, N., Ozenci, V., Fredrikson, S., Link, H., 1999. Interleukin-17 mRNA expression in blood and CSF mononuclear cells is augmented in multiple sclerosis. Mult. Scler. 5 (2), 101–104.

Meeuwsen, S., Persoon-Deen, C., Bsibsi, M., Ravid, R., van Noort, J.M., 2003. Cytokine, chemokine and growth factor gene profiling of cultured human astrocytes after exposure to proinflammatory stimuli. Glia 43 (3), 243–253.

Nitta, A., Ito, M., Fukumitsu, H., Ohmiya, M., Ito, H., Sometani, A., Nomoto, H., Furukawa, Y., Furukawa, S., 1999. 4-methylcatechol increases brain-derived neurotrophic factor content and mRNA expression in cultured brain cells and in rat brain in vivo. J. Pharmacol. Exp. Ther. 291, 1276–1283.

Nitta, A., Nishioka, H., Fukumitsu, H., Furukawa, Y., Sugiura, H., Shen, L., Furukawa, S., 2004. Hydrophobic dipeptide Leu-Ile protects against neuronal death by inducing brain-derived neurotrophic factor and glial cell line-derived neurotrophic factor synthesis. J. Neurosci. Res. 78, 250–258.

Park, H., Li, Z., Yang, X.O., Chang, S.H., Nurieva, R., Wang, Y.H., Wang, Y., Hood, L., Zhu, Z., Tian, Q., Dong, C., 2005. A distinct lineage of CD4 T cells regulates tissue inflammation by producing interleukin 17. Nat. Immunol. 6 (11), 1133–1141.

Pollock, J.S., Forstermann, U., Mitchell, J.A., Warner, T.D., Schmidt, H.H.H.W., Nakane, M., Murad, F., 1991. Purification and characterization of particulate endothelium-derived relaxing factor synthase from cultured and native bovine aortic endothelial cells. Proc. Natl. Acad. Sci. 88, 10480–10484.

Röhn, T.A., Jennings, G.T., Hernandez, M., Grest, P., Beck, M., Zou, Y., Kopf, M., Bachmann, M.F., 2006. Vaccination against IL-17 suppresses autoimmune arthritis and encephalomyelitis. Eur. J. Immunol. 36 (11), 2844–2848.

Sonobe, Y., Yawata, I., Kawanokuchi, J., Takeuchi, H., Mizuno, T., Suzumura, A., 2005. Production of IL-27 and other IL-12 family cytokines by microglia and their subpopulations. Brain Res. 1040 (1–2), 202–207.

Suzumura, A., Mezitis, S.G., Gonatas, N.K., Silberberg, D.H., 1987. MHC antigen expression on bulk isolated macrophage-microglia from newborn mouse brain: induction of Ia antigen expression by gamma-interferon. J. Neuroimmunol. 15 (3), 263–278.

Suzumura, A., Takeuchi, H., Zhang, G., Kuno, R., Mizuno, T., 2006. Roles of glia-derived cytokines on neuronal degeneration and regeneration. Ann. N. Y. Acad. Sci. 1088, 219–229 Review.

Takeuchi, H., Mizuno, T., Zhang, G., Wang, J., Kawanokuchi, J., Kuno, R., Suzumura, A., 2005. Neuritic beading induced by activated microglia is an early feature of neuronal dysfunction toward neuronal death by inhibition of mitochondrial respiration and axonal transport. J. Biol. Chem. 280 (11), 10444–10454.

Towbin, H., Staehelin, T., Gordon, J., 1979. Electrophoretic transfer of proteins from polyacrylamide gels to nitrocellulose sheets: procedure and some applications. Proc. Natl. Acad. Sci. U. S. A. 76 (9), 4350–4354.

Trajkovic, V., Stosic-Grujicic, S., Samardzic, T., Markovic, M., Miljkovic, D., Ramic, Z., MostaricaStojkovic, M., 2001. Interleukin-17 stimulates inducible nitric oxide synthase activation in rodent astrocytes. J. Neuroimmunol. 119, 183–191.

Valdhoen, M., Hocking, R.J., Atkins, C.J., Locksley, R.M., Stockinger, B., 2006. TGFbeta in the context of an inflammatory cytokine milieu supports de novo differentiation of IL-17 producing T cells. Immunity 24, 179–189.

Yao, Z., Painter, S.L., Fanslow, W.C., Ulrich, D., Macduff, B.M., Spriggs, M.K., Armitage, R.J., 1995. Human IL-17: a novel cytokine derived from T cells. J. Immunol. 155 (12), 5483–5486.

0022-3565/08/3271-137–147$20.00
THE JOURNAL OF PHARMACOLOGY AND EXPERIMENTAL THERAPEUTICS
Copyright © 2008 by The American Society for Pharmacology and Experimental Therapeutics
JPET 327:137–147, 2008

Vol. 327, No. 1
141309/3384925
Printed in U.S.A.

The Extensive Nitration of Neurofilament Light Chain in the Hippocampus Is Associated with the Cognitive Impairment Induced by Amyloid β in Mice

Tursun Alkam, Atsumi Nitta, Hiroyuki Mizoguchi, Akio Itoh, Rina Murai, Taku Nagai, Kiyofumi Yamada, and Toshitaka Nabeshima

Department of Neuropsychopharmacology and Hospital Pharmacy, Nagoya University Graduate School of Medicine, Nagoya, Japan (T.A., A.N., H.M., A.I., R.M., T.Nag., K.Y., T.Nab.); Department of Basic Medicine, College of Traditional Uighur Medicine, Hotan, China (T.A.); and Department of Chemical Pharmacology, Graduate School of Pharmaceutical Science, Meijo University, Nagoya, Japan (T.Nab.)

Received May 19, 2008; accepted July 9, 2008

ABSTRACT

Tyrosine nitration of proteins at an extensive level is widely associated with the cognitive pathology induced by amyloid β peptide (Aβ). However, the precise identity and explicit consequences of protein nitration have scarcely been addressed. In this study, we examined the detectable nitration of proteins in the hippocampus of mice with cognitive impairment (day 5) induced by the i.c.v. injection of $A\beta_{25-35}$ (day 0). The intensity of the nitration of proteins was inversely associated with the level of recognition memory in mice. The detectable tyrosine nitrations were revealed in proteins with a single size of approximately 70 kDa. The specific nitrated proteins at this size were identified using the liquid chromatography/mass spectrometry/mass spectrometry analysis and immunodetection methods. Intense nitration of the neurofilament light chain (NFL) was observed. The increased nitration of NFL was associated with its serine hyperphosphorylation and weak interaction with the nuclear distribution element-like, a protein essential for the stable assembly of neurofilaments. No changes in cell numbers in the hippocampus were found (day 5) in mice that received $A\beta_{25-35}$ injections. These findings suggested that extensive nitration of NFL is associated with the Aβ-induced impairment of recognition memory in mice.

Increased nitration of proteins, a surrogate marker of widespread oxidative damage in brains affected by the amyloid β peptide (Aβ), is evidently correlated with the severity of cognitive dysfunction in humans as well as animals (Smith et al., 1997; Lim et al., 2001; Perry et al., 2002; Kim et al., 2003; Andersen, 2004; Bastianetto and Quirion, 2004; Walsh and Selkoe, 2004).

We have previously reported the contribution of tyrosine nitration to Aβ-induced, oxidative damage-mediated cognitive dysfunction in mice (Alkam et al., 2007, 2008). A mouse monoclonal anti-nitrotyrosine antibody in Western blot analysis identified the tyrosine-nitrated hippocampal proteins at approximately 70 kDa as a single band with which the severity of cognitive impairments in mice was well associated (Alkam et al., 2007). In this study, we aimed to identify the nitrated proteins in the single band for the specification of the contribution of the extensive nitration of tyrosine to the cognitive impairment. To produce strong and stable nitrative damage, we applied $A\beta_{25-35}$, a toxic Aβ fragment that is detected in the human brain (Pike et al., 1995; Kubo et al., 2002). The tyrosine-nitrated proteins were examined by using liquid chromatography/mass spectrometry/mass spec-

This work was supported, in part, by the following: Japan-China Sasakawa Medical fellowship (to T.A.); Uehara Memorial Foundation fellowship for Foreign Researchers in Japan (to T.A.); grant-in-aid for the 21st Century Center of Excellence Program "Integrated Molecular Medicine for Neuronal and Neoplastic Disorders" and "Academic Frontier Project for Private Universities (2007–2011)" from the Ministry of Education, Culture, Sports, Science and Technology of Japan; Comprehensive Research on Aging and Health from the Ministry of Health, Labor and Welfare of Japan; Japan-Canada Joint Health Research Program and Japan-France Joint Health Research Program (Joint Project from Japan Society for the Promotion of Science); and International Research Project Supported by the Meijo Asian Research Center.

Article, publication date, and citation information can be found at http://jpet.aspetjournals.org.
doi:10.1124/jpet.108.141309.

ABBREVIATIONS: Aβ, amyloid β peptide; LC-MS/MS, liquid chromatography/mass spectrometry/mass spectrometry; NFL, neurofilament light chain; NUDEL, nuclear distribution element-like; NF, neurofilament; $ONOO^-$, peroxynitrite; UA, uric acid; RIPA, radioimmunoprecipitation assay; PBS, phosphate-buffered saline; PAGE, polyacrylamide gel electrophoresis; PVDF, polyvinylidene difluoride; HSP70, heat shock protein 70; DRP-2, dihydropyrimidinase-like 2; GAPDH, glyceraldehyde 3-phosphate dehydrogenase; SD, sodium dithionite; CBB, Coomassie Brilliant Blue; AD, Alzheimer's disease.

trometry (LC-MS/MS) and immunodetection. Intense nitration of the neurofilament light chain (NFL) was observed. The intensive nitration was associated with serine hyperphosphorylation and reduced interaction of NFL with nuclear distribution element-like (NUDEL), a protein essential for the stable assembly of neurofilaments (NFs). The results provided further support for the conception that extensive nitration of tyrosine in proteins underlies one of the key mechanisms contributing to the cognitive pathology induced by Aβ.

Materials and Methods

Animals. Male ICR mice (Nihon SLC Co., Shizuoka, Japan) were used. The animals were housed in a controlled environment (23 ± 1°C, 50 ± 5% humidity) and allowed access to food and water ad libitum. The room lights were kept on between 8:00 AM and 8:00 PM. All experiments were performed in accordance with the Guidelines for Animal Experiments of Nagoya University Graduate School of Medicine. The procedures involving animals and their care conformed to the *Guidelines for Proper Conduct of Animal Experiments* (Science Council of Japan, 2006).

Treatment and Experimental Design. $A\beta_{25-35}$ (Bachem, Bubendorf, Switzerland) was dissolved in sterile double-distilled water to a stock concentration of 1 mg/ml and stored at −20°C before use. The dissolved $A\beta_{25-35}$ was incubated for aggregation at 37°C for 4 days. The distilled water was incubated at the same conditions and used as the vehicle. $A\beta_{1-40}$ (Bachem) was dissolved to a stock concentration of 1.0 mg/ml in 35% acetonitrile/0.1% trifluoroacetic acid and stored at −20°C before use. The solution of peroxynitrite ($ONOO^-$; 144 mM) (Millipore, Billerica, MA) was stored at −80°C before use. Incubated $A\beta_{25-35}$ (3 μg/3 μl), incubated distilled water (3 μl), $A\beta_{1-40}$ (5 μg/5 μl), and $ONOO^-$ (144 mM/1 μl) were administered by i.c.v. injection as described previously (Maurice et al., 1996; Alkam et al., 2007, 2008). In brief, a microsyringe with a 28-gauge stainless steel needle 3.0-mm long was used for all experiments. Mice were anesthetized lightly with ether, and the needle was inserted unilaterally 1 mm to the right of the midline point equidistant from each eye, at an equal distance between the eyes and the ears and perpendicular to the plane of the skull. A single shot of the indicated volume of agents was delivered gradually within 3 s. Mice exhibited normal behavior within 1 min after the injection. The injection placement or needle track was visible and was verified at the time of dissection. Neither insertion of the needle nor the volume of injection had a significant influence on survival, behavioral responses, or cognitive functions. Uric acid (UA) (Wako Pure Chemicals, Osaka, Japan) was prepared as a suspension in saline. Immediately after the single injection of $A\beta_{25-35}$ or $A\beta_{1-40}$, mice were given UA (100 mg/kg i.p.) daily for 6 consecutive days. The schedule of administration of peptides and drugs as well as biochemical, histochemical, and behavioral investigations is shown in Fig. 1.

Novel Object Recognition Task. This task, based on the spontaneous tendency of rodents to explore a novel object more often than a familiar one, was performed on days 3 to 5 after the i.c.v. injection of $A\beta_{1-40}$, $A\beta_{25-35}$, or peroxynitrite (day 0) as described previously (Alkam et al., 2007). A plastic chamber (35 × 35 × 35 cm) was used in low light conditions during the light phase of the light/dark cycle. The general procedure consisted of three different phases: 1) a habituation phase, 2) an acquisition phase, and 3) a retention phase. On the 1st day (habituation phase), mice were individually subjected to a single familiarization session of 10 min, during which time they were introduced into the empty arena to become familiar with the apparatus. On the 2nd day (acquisition phase), the animals were subjected to a single 10-min session, during which time two floor-fixed objects (A and B) were placed in a symmetric position from the center of the arena, 15 cm from each other and 8 cm from the nearest wall. The two objects, made of the same wooden material with a similar color and smell, were different in shape but identical in size. Mice were allowed to explore the objects in the open field. A preference index for each mouse was expressed as a ratio of the amount of time spent exploring object A (TA × 100)/(TA + TB), where TA and TB are the time spent exploring object A and object B, respectively. On the 3rd day (retention phase), mice were allowed to explore the open field in the presence of two objects: the familiar object A and a novel object C in different shapes but in similar color and size (A and C). A recognition index, calculated for each mouse, was expressed as the ratio (TC × 100)/(TA + TC), where TA and TC are the time spent during the retention phase on object A and object C, respectively. The time spent exploring the object (nose pointing toward the object at a distance ≤ 1 cm) was recorded by hand.

Sample Preparation. Animals were decapitated, and the hippocampi were removed on an ice-cold glass plate and stored at −80°C. Hippocampal protein extracts were obtained by homogenization in diverse ice-cold lysis buffers that included the radioimmunoprecipitation assay (RIPA) buffer, phosphate-buffered saline (PBS) buffer, Triton X-100 buffer, and 6 M urea buffer. The RIPA lysis buffer contained 20 mM trizma hydrochloride, pH 7.6, 150 mM sodium chloride, 2 mM EDTA·2Na, 50 mM sodium fluoride, 1 mM sodium vanadate, 1% Nonidet P-40, 1% sodium deoxycholate, 0.1% SDS, 1 mg/ml pepstatin, 1 mg/ml aprotinin, and 1 mg/ml leupeptin. The PBS lysis buffer, pH 7.4, contained 135 mM sodium chloride, 3.2 mM disodium hydrogen phosphate 12-water, 1.3 mM potassium chloride, and 0.5 mM potassium dihydrogen phosphate. The Triton X-100 buffer contained 10 mM trizma hydrochloride at pH 7.5, 150 mM sodium chloride, 1 mM EDTA at pH 8.0, and 1% Triton X-100. The 6 M urea lysis buffer contained 10 mM trizma base at pH 8.1, 6 M urea, and 1 mM dithiothreitol. All of these lysis buffers, with the exception of the RIPA buffer, were supplemented with complete protease inhibitor cocktail tablets (Roche Applied Science, Mannheim, Germany). Homogenates were centrifuged at 13000*g* for 20 min to obtain the desired supernatant of the extracts. The centrifuged pellets were washed twice with the previous buffer before being solubilized. The washing procedure consisted of complete dispersion of the pellets by vortexing and incubation in ice for 30 min followed by centrifugation at 13000*g* for 20 min. The unassembled NFL and NUDEL proteins were obtained within the soluble proteins in Triton X-100 buffer (Nguyen et al., 2004), and the insoluble protein pellets that include the assembled NFL and NUDEL proteins were then solubilized in 6 M urea lysis buffer (Crow et al., 1997). The cytoplasmic water-soluble proteins were obtained in PBS lysis buffer (Aoyama and Kitajima, 1999), and the insoluble pellets were then solubilized in Triton X-100 buffer. The concentrations of PBS-soluble and urea-soluble proteins were determined with a Bio-Rad protein assay reagent kit (Bio-Rad, Hercules, CA). The concentrations of the Triton

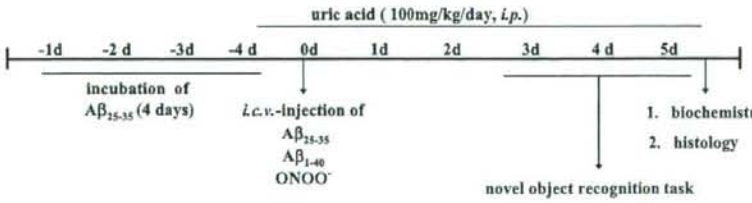

Fig. 1. The experimental design of the study.

X-100-soluble proteins were determined with a BCA protein assay reagent kit (Pierce, Rockford, IL).

Western Blot Analysis. Equal amounts (20 μg) of protein sample were resolved by a 4 to 20% gradient or 7% SDS-polyacrylamide gel electrophoresis (PAGE). The proteins were then transferred electrophoretically to a polyvinylidene difluoride (PVDF) membrane (Millipore). Membranes were incubated in 3% skim milk or 3% bovine serum albumin (for phosphor-protein) in phosphate-buffered saline containing 0.05% (v/v) Tween 20 for 2 h at room temperature. Anti-nitrotyrosine mouse monoclonal 1A6 antibody (catalog number 05-233; Millipore), anti-NFL mouse antibody (Sigma-Aldrich, St. Louis, MO), anti-heat shock protein 70 (HSP70) polyclonal antibody (Assay Designs, Ann Arbor, MI), anti-dihydropyrimidinase-like 2 (DRP-2) mouse antibody (IBL, Takasaki, Japan), anti-NUDEL rabbit antibody (Abcam Inc., Cambridge, MA), anti-phosphoserine rabbit antibody (Zymed Laboratories, South San Francisco, CA), anti-β-actin goat antibody (Santa Cruz Biotechnology Inc., Santa Crutz, CA), and anti-glyceraldehyde 3-phosphate dehydrogenase (GAPDH) mouse antibody (Imgenex, San Diego, CA) were used. To confirm the specificity of the detected single band of tyrosine-nitrated proteins, the reduction of nitrotyrosine to aminotyrosine was performed. In brief, the membrane was treated with 10 mM sodium dithionite (SD) in 50 mM pyridine-acetate buffer, pH 5.0, for 1 h at room temperature. After the reaction, the membrane was rinsed with distilled water and then equilibrated with washing buffer and blocked for 1 h at room temperature in blocking solution before standard procedures of Western blotting were followed. The absent band in the SD-treated membrane compared with the routine-treated control membrane was regarded to be a genuine for nitrated proteins. To confirm the specificity of the detected band for phosphoserine, the anti-phosphoserine inhibitor (the inhibitor) that contains phosphoserine was used to block the specific interaction of anti-phosphoserine primary antibodies with serine-phosphorylated proteins in the membrane. In brief, the anti-phosphoserine primary antibody and the inhibitor at a final concentration of 20 mM were mixed into a bovine serum albumin-containing blocking buffer and preincubated for 10 min for the ample binding of the antibodies with the phosphoserines (to cover up all of the specific anti-phosphoserine antibodies) before the application to the membrane. Incubation of the antibody-inhibitor mixture with the membrane was carried out for 1 h at room temperature. After the incubation, standard procedures were followed for blot washing and incubation with a secondary antibody. The absence of the bands in the membrane after the antibody-inhibitor treatment compared with the membrane subjected to routine treatment was regarded as genuine proof of serine phosphorylation. The intensity of each protein band on the film was analyzed with the Atto Densitograph 4.1 system (Atto, Tokyo, Japan) and was corrected with the corresponding β-actin or GAPDH level. The results were expressed as a percentage of that in the naive group.

Liquid Chromatography/Mass Spectrometry/Mass Spectrometry. Protein bands in the SDS-PAGE were stained with Coomassie Brilliant Blue (CBB) (Fluka, Buchs, Switzerland). The band of interest was excised from the gel. The gel piece was digested in trypsin solution at 35°C for 20 h for analysis by LC/MS/MS (Aproscience Lifescience Institute, Tokushima, Japan).

Immunoprecipitation. Hippocampal homogenates for Western blottings were used for immunoprecipitation. The antibodies against the proteins of interest were incubated overnight with 50 μl of protein A-Sepharose beads (GE Healthcare, Little Chalfont, Buckinghamshire, UK). To obtain tyrosine-nitrated proteins, anti-nitrotyrosine agarose-conjugated mouse antibody (Millipore) was used. The bead-antibody complexes were incubated overnight with 500 μg of precleared proteins in the corresponding buffers, with the exception that urea lysis buffer does not include dithiothreitol. Immunocomplexes were collected by centrifugation at 13000*g* for 1 min at 4°C and then washed three times with ice-cold PBS. Immunoprecipitated samples were recovered by resuspending in 2× sample loading buffer, immediately fractionated by reducing in 7% SDS-PAGE, and analyzed by Western blotting with the corresponding antibodies.

Histology. Each mouse was anesthetized with diethyl ether and quickly intracardially perfused with physiological saline followed by 4% paraformaldehyde in 100 mM PBS, pH 7.4. The brains were quickly removed, postfixed for 24 h in the same fixative solution, and cryoprotected in a graded 10 to 40% sucrose solution in 100 mM PBS. Coronal sections were cut 20-μm thick using a cryostat (Leica, Wetzlar, Germany) and stained with 0.1% cresyl violet reagent (Wako Pure Chemicals) according to standard procedures. The sections were mounted in fluorescent medium (Dako North America, Inc., Carpinteria, CA), and images of CA1, CA3, and the granular layer of the dentate gyrus of the hippocampus were taken using a Carl Zeiss Axioskop phase-contrast microscope with a cooled CCD camera system (SenSys; Photometrics Ltd., Tucson, AZ). The Nissl-positive neuronal cells were counted using Image J software (version 1.38; National Institutes of Health, Bethesda, MD). The total cell count in per millimeter square was averaged from four sections per animal ($n = 4$) according to previous reports (Nabeshima et al., 1991; Nitta et al., 1997).

Statistical Analysis. The results are expressed as the mean ± S.E. Statistical significance was determined with a one-way analysis of variance followed by the Bonferroni multiple comparisons test. $p < 0.05$ was taken as a significant level of difference.

Results

The Tyrosine Nitration of Proteins Induced by $A\beta_{25-35}$ in the Hippocampus of Mice. Anti-nitrotyrosine mouse antibody detected only a single band of hippocampal proteins at approximately 70 kDa for tyrosine nitration, which induced a potent nitrating agent after the i.c.v. injection of $A\beta_{1-40}$, $A\beta_{25-35}$, and peroxynitrite ($ONOO^-$) (Fig. 2A). Aβ peptides induced extensive nitration of proteins in the hippocampus and impairment of recognition memory, both of which were prevented by UA, a potent scavenger of $ONOO^-$. $ONOO^-$ induced marked tyrosine nitration of proteins in the hippocampus and impairment of recognition memory (Fig. 2, B and C). The intensity of the nitration was inversely associated with the recognition memory in mice (Fig. 2D). The authenticity of nitration was confirmed by the reduction of nitrotyrosine to aminotyrosine with SD in the membrane and by detecting the nitrotyrosine using the same antibody. The absence of this band after SD treatment was regarded as a genuine band for proteins with tyrosine nitration (Fig. 2, E and F). Proteins in SDS-PAGE were stained with CBB, and the 70-kDA protein band was excised for identification (Fig. 2G). The proteins in the excised gel were in-gel-trypsin-digested and subjected to LC/MS/MS, and several proteins were successfully identified (Table 1).

The Identification of the Tyrosine-Nitrated Proteins and the Level of Nitration. The nitration of the identified proteins was examined by applying the immunoprecipitation method. For peptide match scores, HSP70, DRP-2, and NFL were favored for the further study. Because the antibody that was used to detect the nitrated proteins in Western blot analysis could not be used for immunoprecipitation, a specially designed agarose-conjugated mouse anti-nitrotyrosine monoclonal antibody was used. We applied $A\beta_{25-35}$ for the rest of the study, considering its property to produce stronger and stable oxidative damage (Pike et al., 1995) as evidenced in Fig. 2. Immunoprecipitated nitrated-proteins were fractionated by SDS-PAGE and blotted with the antibodies raised against the proteins of interest (Fig. 3A). Intensive

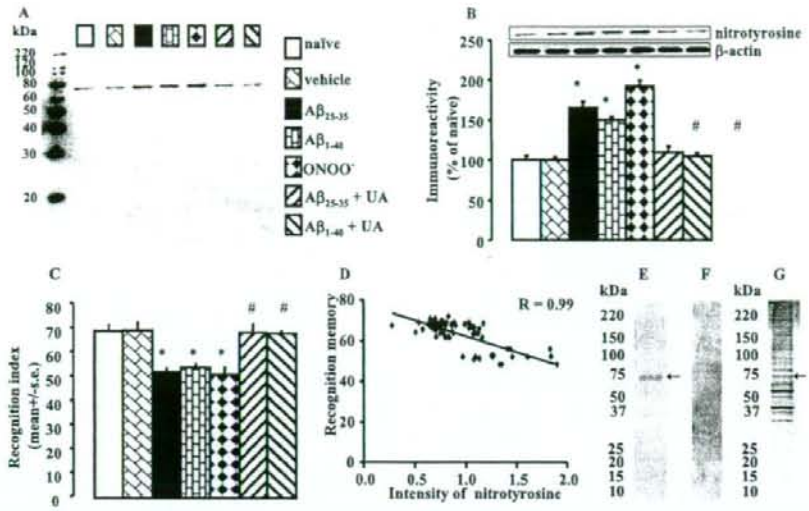

Fig. 2. The tyrosine nitration of proteins in the hippocampus and the cognitive function in mice. A and B, nitrotyrosine in the hippocampus was measured 5 days after the i.c.v. injection of Aβ peptides or $ONOO^-$. Protein samples from the hippocampus were subjected to SDS-PAGE, blotted to a PVDF membrane, and probed with a monoclonal anti-nitrotyrosine antibody. Aβ peptides induced extensive nitration of protein, which was prevented by UA, a potent scavenger of $ONOO^-$. $ONOO^-$ induced marked tyrosine nitration of proteins. The quantified intensity of the bands for nitrotyrosine was corrected by that of β-actin and expressed as a percentage of that in the naive group. Data are presented as the mean ± S.E. (n = 4). *, $p < 0.05$ versus naive and vehicle; #, $p < 0.05$ versus $A\beta_{25-35}$ or $A\beta_{1-40}$. C, the novel object recognition task was performed on days 3 to 5 after the i.c.v. injection of Aβ peptides or $ONOO^-$. Aβ peptides induced marked impairments of recognition memory, which were prevented by UA. $ONOO^-$ induced impairment of recognition memory. Data are presented as the mean ± S.E. (n = 10). *, $p < 0.05$ versus naive and vehicle; #, $p < 0.05$ versus $A\beta_{25-35}$ and $A\beta_{1-40}$. D, the panel shows the inverse association of extensive nitration of protein tyrosine in the hippocampus and the level of recognition memory in mice. E and F, protein samples from the hippocampus were subjected to 4 to 20% SDS-PAGE, blotted to PVDF membrane, and probed with a monoclonal anti-nitrotyrosine antibody before (E) and after (F) reduction of nitrotyrosine to aminotyrosine by treating the membrane with SD. G, protein bands in 4 to 20% SDS-PAGE were stained by CBB, and the band of interest was picked up for peptide analysis using LC-MS/MS.

TABLE 1
The identified protein candidates

Protein Name	gi Accession Number	Peptide Matched	% Sequence Coverage	Total Score
HSP70	gi 1661134	22	39	724
DRP-2	gi 40254595	7	20	292
NFL	gi 200038	4	9	254
ATPase, H^+transporting, V1 subunit A, isoform 1	gi 315607	9	17	184
Glycerol-3-phosphate dehydrogenase	gi 1339938	1	2	96
Ig superfamily receptor PGRL	gi 15593237	1	3	55
Solute carrier family 25 (mitochondrial carrier, aralar member12)	gi 27369581	3	8	53

gi, genInfo identifier; PGRL, prostaglandin regulatory-like protein.

nitration was observed for NFL in the $A\beta_{25-35}$ group compared with the naive or vehicle group (Fig. 3, A and B). No differences were observed in the nitration of HSP70 and DRP-2 proteins among the three groups (Fig. 3, A, C, and D). The increased nitration of NFL was inversely associated with recognition memory in mice that received $A\beta_{25-35}$ injections (Fig. 3E).

Association between Extensive Nitration of NFL and Serine Hyperphosphorylation. Hyperphosphorylation of the serine residues of NFL could lead to disruption of the subtle regulation of the NF network (Hisanaga et al., 1990; Nixon and Shea, 1992). After being nitrated in vitro, NFL is not able to form the NF assembly (Crow et al., 1997). The question of whether extensive nitration of NFL influences serine phosphorylation of the protein stimulated our interest. We immunoprecipitated NFL and blotted against nitrotyrosine and phosphoserine. Equal amounts of NFL protein were immunoprecipitated in each group (Fig. 4, A and B). The intensity of the tyrosine nitration and serine phosphorylation of NFL was greater in the $A\beta_{25-35}$ group than in the naive or vehicle group (Fig. 4, A, C, and D). The authenticity of the phosphoserine band was confirmed as indicated under *Materials and Methods*. Treatment with UA prevented the $A\beta_{25-35}$-induced intensive tyrosine nitration and serine hyperphosphorylation of NFL (Fig. 4, A, C, and D), indicating a positive association between the extensive nitration of NFL and the serine hyperphosphorylation (Fig. 4E).

Association between Extensive Nitration of NFL and Its Reduced Interaction with NUDEL. To examine whether the extensive nitration of NFL practically influences its interaction with partner proteins, we focused on the free, unassembled NFL that could be differentiated from the assembled NFL. The majority of the newly synthesized unassembled NF proteins, including NFL, are Triton X-100-solu-

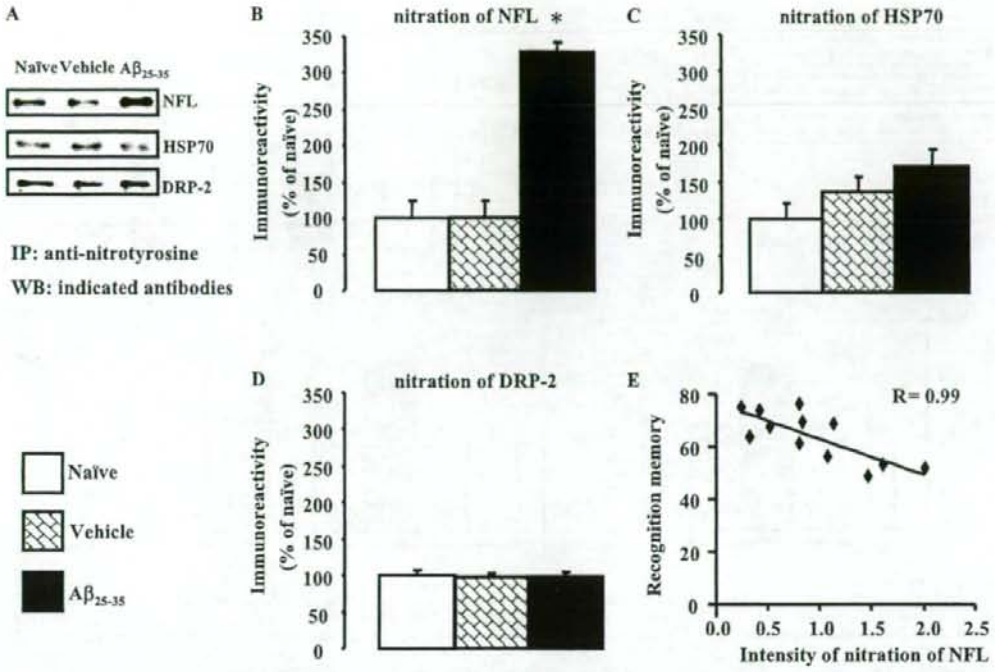

Fig. 3. Tyrosine nitration of the identified proteins. A, immunocomplexes, obtained from precleared protein samples of the hippocampus using an anti-nitrotyrosine agarose-conjugated mouse antibody, were separated by 7% SDS-PAGE, blotted onto a PVDF membrane, and probed with corresponding antibodies raised against the proteins of interest. B to D, NFL was intensely nitrated in the $A\beta_{25-35}$ group, whereas HSP70 and DRP-2 remained unchanged. E, the panel shows inverse association of the extensive nitration of NFL in the hippocampus (B) and the level of recognition memory in mice (Fig. 1B). The intensity of bands was quantified and expressed as a percentage of that in the naive group. Data are presented as the mean ± S.E. ($n = 4$). *, $p < 0.05$ versus naive and vehicle.

ble before being incorporated into the NF assembly, which is Triton X-100-insoluble (Black et al., 1986). NFL constitutes the core of the NF network, and without NFL, no filaments are formed (Zhu et al., 1997). Without binding directly with NUDEL, the Triton X-100-soluble NFL can barely lead the assembly of a stable NF network, regardless of its own abundance (Nguyen et al., 2004). We probed equal amounts of NFL immunocomplexes with antibodies raised against the nitrotyrosine and NUDEL (Fig. 5, A and B). Less NUDEL was coimmunoprecipitated in the $A\beta_{25-35}$ group that bears extensively nitrated NFL (Fig. 5, A–D). The protein expression of NUDEL did not differ among the groups (Fig. 5E). UA prevented the $A\beta_{25-35}$-induced increase of NFL nitration as well as the reduced coimmunoprecipitation of NUDEL (Fig. 5, A, C, and D). The extensive nitration of NFL was associated with its reduced interaction with NUDEL (Fig. 5F). These results suggested that the intensive nitration of NFL could disturb the normal function of the protein.

Association between Extensive Nitration of NFL and the Reduced Content of NUDEL in the Cytoskeleton Fraction. A majority of NF proteins, after their synthesis in the cytoplasm, are rapidly converted to a Triton X-100-insoluble filamentous network and move down the axon using the transport machinery (Nixon and Shea, 1992). After direct and specific binding with NFL, NUDEL facilitates the assembly of a stable NF network and remains bound to the assembled filaments (Nguyen et al., 2004). Thus, the level of interaction between NFL and NUDEL in cytoplasm (Triton X-100-soluble fraction) should be reflected by their protein levels in the axonal cytoskeleton (Triton X-100-insoluble fraction). The Triton X-100-insoluble fractions from the previous step (Fig. 5) were washed twice with Triton X-100 lysis buffer before being solubilized in urea lysis buffer. Western blot analysis revealed that the level of NUDEL protein was reduced in the $A\beta_{25-35}$ group compared with the naive and vehicle groups, whereas the treatment with UA prevented the reduction (Fig. 6, A and D). This was consistent with the reduced interaction between NFL and NUDEL in the $A\beta_{25-35}$ group (Fig. 5, A and D). However, the level of NFL in the $A\beta_{25-35}$ group was surprisingly not different from that in the naive and vehicle groups (Fig. 6, A and B). Considering the increase of the intensity of the protein nitration in the $A\beta_{25-35}$ group (Fig. 6, A and C), we examined the nitration of NFL by immunoprecipitation. Intense nitration for the NFL protein in the $A\beta_{25-35}$ group was observed (Fig. 6E). Applying the multiplicative inverse (in which the inverse or reciprocal of "n" is "1/n"), a mathematical method that is useful in medical science (Silberberg, 1990), the reciprocal level of the extensively nitrated NFL in the Triton X-100-insoluble fraction was estimated (Fig. 6F). The reciprocal level of extensively nitrated NFL in the $A\beta_{25-35}$ group paralleled with that of NUDEL in the same group (Fig. 6, D and F), signifying a negative effect of the extensive nitration of NFL on NUDEL-dependent NF assembly. The increased nitration of tyrosine could modify protein function by altering the three-dimensional conformation and hydrophobicity (Dalle-Donne et al.,

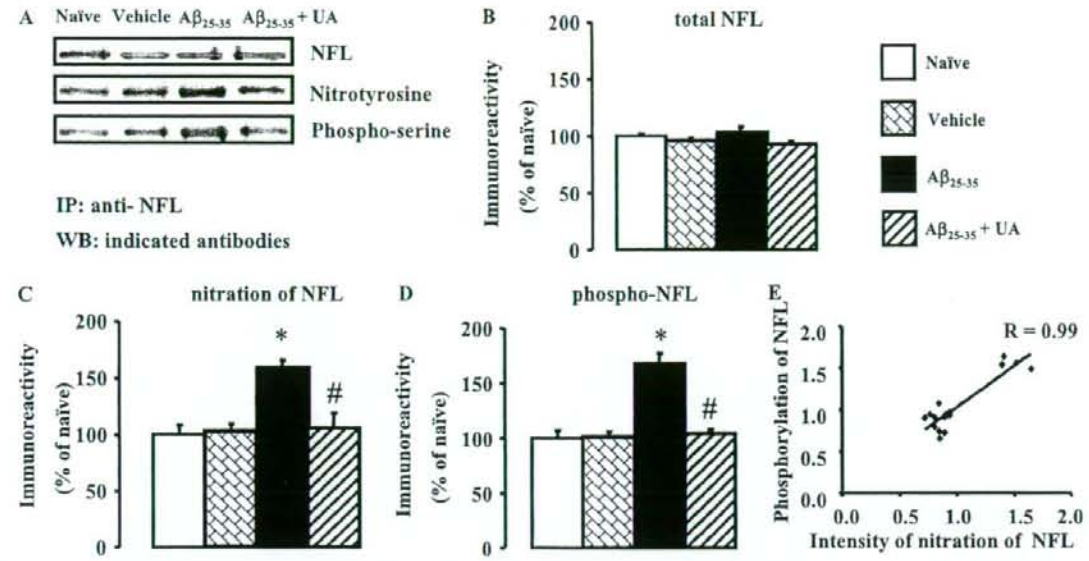

Fig. 4. The association between the increased tyrosine nitration and serine hyperphosphorylation of NFL. A, equal amounts of NFL protein immunocomplexes were obtained from precleared protein samples of the hippocampus, using anti-NFL antibody. The immunocomplexes were separated on SDS-PAGE, blotted onto a PVDF membrane, and probed with the indicated antibodies. B to D, tyrosine nitration and serine phosphorylation of NFL were increased in the $A\beta_{25-35}$ group, whereas UA prevented the increase of both. E, the increased nitration of NFL was correlated with serine hyperphosphorylation of NFL. The intensity of bands was quantified and expressed as a percentage of that in the naive group. Data are presented as the mean ± S.E. ($n = 4$). *, $p < 0.05$ versus naive and vehicle; #, $p < 0.05$ versus $A\beta_{25-35}$.

2005; Reynolds et al., 2007). It was therefore assumed that the overnitrated, free NFL would become less Triton X-100 soluble and, as a result, would be detected in the Triton X-100-insoluble fraction along with the assembled NF proteins. It is hardly practical to separate the unassembled extensively nitrated NFL from the assembled NFL in the Triton X-100-insoluble fraction. The majority of the cytoplasmic water-soluble proteins could be separated from the Triton X-100-soluble protein pools by using PBS lysis buffer in the first step (Aoyama and Kitajima, 1999). After the separation of the PBS-soluble and Triton X-100-soluble proteins as described under *Materials and Methods*, we examined the amount of NFL protein in these two different fractions. The majority of NFL protein in all groups was found in the PBS-soluble cytoplasmic fraction as indicated by GADPH, a cytoplasmic marker (Fig. 7A). The levels of NFL protein in both the PBS-soluble and Triton X-100-soluble fractions were increased in the $A\beta_{25-35}$ group (Fig. 7, A–C). It is interesting to note that the increase of NFL in both fractions was prevented by the treatment with of UA, a potent scavenger of $ONOO^-$, suggesting that the $A\beta_{25-35}$-induced $ONOO^-$ may increase the protein synthesis of NFL before extensively nitrating the protein (Fig. 7, A–C). The Triton X-100-soluble NFL that became insoluble in PBS in the $A\beta_{25-35}$ group was extensively nitrated (Fig. 7D), and the intensity of nitration was associated with the level of the PBS-insoluble, Triton X-100-soluble NFL (Fig. 7E). These results revealed new possibilities for Triton X-100-insolubile NFL in association with extensive nitration.

The Cell Numbers in the Hippocampus of Mice with the Impairment of Memory Induced by $A\beta_{25-35}$. On day 5 after the i.c.v. injection of $A\beta_{25-35}$, cell numbers in CA1, CA3, and the granular layer of the dentate gyrus of the hippocampal formation were examined using cresyl violet staining. The quantification of the stained cells revealed no cell loss induced by $A\beta_{25-35}$ (Table 2). These results were consistent with reports that at a dose of 3 to 5 μg, $A\beta_{25-35}$ could induce memory impairment but not cell loss within a time session of 1 month after its injection in mice (Maurice et al., 1996; Tohda et al., 2003). These results suggest that cell loss was not involved in the impairment of memory induced by $A\beta_{25-35}$ in mice.

Discussion

Neuronal oxidative damage has long been hypothesized as a critical mechanism of cellular dysfunction in neurodegenerative ailments (Perry et al., 2002). Reports showing that antioxidants delay or reduce progressive cognitive decline in both animal models and humans have emphasized the direct contribution of oxidative damage to cognitive pathology (Sano et al., 1997; Yamada et al., 1999; Lim et al., 2001). Oxidative damage is generally manifested by the increase of lipid peroxidation, DNA oxidation, protein oxidation, and peroxynitrite-mediated tyrosine nitration of proteins. The increased nitration of tyrosine could irreversibly disrupt the function of proteins (Koppal et al., 1999), and it might play a key pathogenic role in the progression of cognitive impairment (Smith et al., 1997; Keller, 2006). Until now, various proteins with tyrosine nitration have been reported in association with neurodegeneration and cognitive decline (Strong et al., 1998; Castegna et al., 2003; Tran et al., 2003; Sacksteder et al., 2006; Sultana et al., 2006). The diversity of nitrated proteins in these reports seems to depend on the species of the sources of samples (Sacksteder et al., 2006;